Eocene biogeochronology and magnetostratigraphic revision of ODP Hole 762C, Exmouth Plateau (northwest Australian Shelf)

Jamie L. Shamrock[1,2,*], David K. Watkins[1], Kurt W. Johnston[2]

[1] *University of Nebraska-Lincoln, Department of Earth and Atmospheric Sciences, Lincoln NE, 68588*

[2] *ExxonMobil Exploration Co., Houston TX, 77060*

email: jamie.shamrock@huskers.unl.edu; dwatkins1@unl.edu; kurt.w.johnston@exxonmobil.com

ABSTRACT: We present a chronostratigraphic model for the Eocene from ODP Leg 122 Hole 762C (northwest Australian shelf), integrating calcareous nannofossil data with previously published planktonic foraminiferal data, magnetostratigraphy and stable isotopic data. This ~240m thick interval extends from magnetic polarity Chron C25r to Chron C15r, and nannofossil zones CP6/7 to CP16a (NP7/8-NP21). Examination of the calcareous nannofossil biostratigraphy showed several potential hiatuses within this stratigraphic section at Hole 762C. The presence of these hiatuses was supported by cross-correlation of planktonic foraminiferal P-zones, magnetostratigraphic reversals and $\delta^{13}C$ and $\delta^{18}O$ isotopic excursions. These biostratigraphic and isotopic data were used to re-evaluate the original magnetostratigraphy, and this revised framework was integrated into a new age model. The original depositional model from Leg 122 proposed a continuous section with relatively low sedimentation rates in the Lutetian and basal Ypresian (< 1.0cm/ky); however, our results suggest that sedimentation rates were relatively high but that the section is interrupted by four hiatuses, each ~1-2 myr in duration. This new age model allowed revision of sedimentation rates at Hole 762C. These revised rates are used to estimate the ages of calcareous nannofossil bioevents, which are compared to several additional, globally distributed localities.

Keywords: geochronology, biostratigraphy, calcareous nannofossils, Eocene, Indian Ocean, ODP Leg 122

INTRODUCTION

The geologic time scale has seen significant evolution since the original interpretation of Hole 762C in 1992. The geomagnetic polarity time scale of Cande and Kent (1995, CK95) and the resultant integrated magnetobiochronologic scale of Berggren et al. (1995a, BKSA95) significantly refined the resolution and reduced many errors of the geologic time scale. Both of these calibrated scales had significant influence on the geologic time scales of Gradstein Ogg and Smith (2004) and Ogg Ogg and Gradstein (2008). In addition to the increased control of microfossil bioevents and magnetic polarity reversals, there has been significant improvement in the resolution of $\delta^{13}C$ and $\delta^{18}O$ isotope stratigraphy through the Eocene (Bohaty et al. 2009; Cramer et al. 2009; Sluijs et al. 2008; Jovane et al. 2007; Nicolo et al. 2007; Lourens et al. 2005; Bohaty and Zachos 2003; Cramer et al. 2003; Zachos et al. 2001; Salamy and Zachos 1999). The progress within these individual disciplines, and with the integration of the different types of stratigraphic data, has changed the way a particular succession may be evaluated. In general, there has been a tendency to assume that many deep sea successions were continuous, particularly in passive geologic settings with high accommodation; however, in the last 20 years, particularly since Berggren et al. (1995a), integration of these biostratigraphic, isotopic, and magnetostratigraphic data have shown how incomplete many of deep-sea successions truly are (Florindo and Roberts 2005; Aubry 1995; Gradstein 1992).

*Corresponding author's present address: ExxonMobil Exploration Co Post Office Box 4778, Houston TX, 77210-4778;
email: jamie.l.shamrock@exxonmobil.com

Ocean Drilling Program (ODP) Leg 122 Hole 762C (northwest Australian Shelf) was selected for a previous study of Eocene calcareous nannofossils (Shamrock and Watkins *this volume*), as aspects of the stratigraphic record were constrained by previous biostratigraphic data (Siesser and Bralower 1992) and depositional models (Golovchenko Borella and O'Connell 1992; Haq et al. 1992), which proposed an essentially complete Eocene record. Reexamination of the calcareous nannofossil biostratigraphy by Shamrock and Watkins (*this volume*) showed several potential hiatuses within this "continuous" section. Attempts to ameliorate these issues through cross-correlation of planktonic foraminifera P-zones, magnetostratigraphic reversals and isotopic excursions further supported the presence of these hiatuses. The present research was conducted to fulfill the need for a new, integrated age model for Hole 762C.

Biostratigraphic, magnetostratigraphic, and isotopic data were published in the Leg 122 *Initial Reports* (Haq Rad and O'Connell 1990) and *Scientific Results* (Rad et al. 1992); however, these data sets had not yet been fully integrated to produce a robust chronostratigraphic framework.

Galbrun (1992) used calcareous nannofossil data of Siesser and Bralower (1992) to guide the magnetostratigraphic interpretation, but issues of core recovery (and undetected hiatuses) limited this interpretation. As noted by Berggren et al. (1995b), Hole 762C does represent a well preserved and expanded Eocene section; however, data from this site was not used in calibration of the Berggren et al. (1995b) integrated magnetobiochronologic scale (IMBS) (hereafter referred to as BKSA95), as the authors believed the data of Galbrun (1992) should be reinterpreted. Though some issues do exist with the

interpretation of Galbrun (1992), we believe many of these can be resolved with integration of additional nannofossil events, as well as planktonic foraminiferal and isotopic data from Hole 762C.

Recent and substantial interest in the chemostratigraphy of the Cenozoic has produced high-resolution $\delta^{13}C$ and $\delta^{18}O$ isotopic records for the Eocene (Galeotti et al. 2010; Bohaty et al. 2009; Pearson et al. 2008; Jovane et al. 2007; Lourens et al. 2005; Bohaty and Zachos 2003; Cramer et al. 2003; Zachos et al. 2001, others). Several isotopic excursions identified in these records have been linked to significant short- and long-term paleoenvironmental changes. When Hole 762C was originally drilled in 1990 these distinct $\delta^{13}C$ and $\delta^{18}O$ excursions, and the associated environmental events, were just recently described (PETM, Paleocene Eocene Thermal Maximum), or had not yet been identified (ETM2, Eocene Thermal Maximum 2). Today these events are not only readily identified and better understood, but have been dated by several groups of researchers, providing another set of calibration points that can be integrated with magnetostratigraphic and biostratigraphic data.

In general, key events near the base (PETM) and top (Oi-1) of the Eocene are fairly well understood; however, the general magneto-biochronology of this epoch is still being developed. In addition, the relationships among paleontologic, magnetostratigraphic, and isotopic events, as well as their relationships to local and regional hiatuses, are still being determined. Integration of various data sets from Leg 122 Hole 762C may help to increase this understanding, particularly in the eastern Indian Ocean.

Here we reinterpret the original magnetostratigraphy from Hole 762C (Galbrun 1992) and integrate this data with the biostratigraphic (Shamrock and Watkins *this volume*) and isotopic data sets (Thomas Shackleton and Hall 1992) in order to develop a more robust geochronology for this locality. Though no stratigraphic breaks were originally identified in Hole 762C, this new interpretation suggests at least four hiatuses, within magnetozones C20n-C20r, C21n-C21r, C22r, and C24r, each 1-2 myr in duration. Uncompacted sedimentation rates derived from this revised age model are used to date significant nannofossil events, and these are compared to dates provided by, or derived from, several additional localities.

SITE LOCALITY AND SAMPLE MATERIAL

ODP Leg 122 Hole 762C

ODP Leg 122 Hole 762C (19°53.23S, 112°15.24E) is located on the central Exmouth Plateau (northern Carnarvon Basin, Australia) and is separated from the Australian Northwest Shelf by the Kangaroo Syncline (Rad et al. 1992) (text-figure 1). Though rifting stretched the site in its early history, the plateau has been relatively inactive since the mid-Cretaceous. The plateau shows fairly uniform thermal subsidence, with decompacted burial curves showing little change in depth since the time of original deposition (Haq et al. 1992).

Hole 762C was drilled in 1360m of water with ~ 240m of Eocene sediments penetrated in Cores 3-29, ~180-422 meters below sea floor (mbsf). Core recovery varies considerably throughout this interval, ranging from 12 to = 100%, with an average recovery of ~67% (text-figure 2). Eocene pelagic sediments from this locality indicate a mature, open-ocean setting (Rad et al. 1992), and are divided into three lithologic subunits: Unit II [3-3-(0cm)-12-1-(0cm)] is composed of white nannofossil chalk and extends from 181.5-265.0 mbsf. Unit IIIA [12-1-(0cm)-26-10-(0cm)] extends from 265.0-398.0 msbf and is composed of light green-grey and white nannofossil chalk with foraminifera. Unit IIIB [26-10-(0cm)-29-1-(50cm)] extends from 398.0-554.8 msbf and consists of light green nannofossil chalk. Both clay content and bioturbation increased downward toward the Lower Eocene.

Additional sites

The dates of calcareous nannofossil events derived from Hole 762C are compared to several additional global localities, particularly for bioevents that have not been calibrated in the BKA95 model. Localities were selected for a well preserved and diverse nannofossil assemblage that provided good biostratigraphic control and for the quality and completeness of magnetostratigraphic data. In an attempt to avoid difficult or ambiguous correlations, we exclude localities with issues that may compromise the stratigraphic interpretation, such as poor nannofossil preservation, weak magnetization, poor core recovery, or identified hiatuses. Localities were also selected for a broad global distribution, at various paleolatitudes and from several ocean basins (text-figure 1). These additional localities are discussed briefly below.

The classic Italian sections of Possagno, Bottaccione, and Contessa Highway are included for comparison of nannofossil events to outcrop data. Biostratigraphic and magnetic polarity data for the Possagno section (45°50’02’’N, 11°31’01’’E) is from Agnini et al. (2006). Magnetostratigraphic data for the Bottaccione section is from Napoleone et al. (1983) and from Lowrie et al. (1982) for the Contessa Highway section. Calcareous nannofossil data for the Bottaccione and Contessa Highway sections are from Monechi and Thierstein (1985). Bottaccione data above C18n from Fornaciari et al. (2011). Additional land-based correlations are derived from the Alano section (NE Italy) (Agnini et al. 2010) and from the New Jersey coastal plain (Miller et al. 1990).

ODP Hole 1051A (Blake Nose) is located in the northwestern Atlantic Ocean (30°03.174’N, 76°21.458’W), and was drilled during Leg 171B. Calcareous nannofossil data are from Mita (2001) with magnetostratigraphic correlations of Ogg and Bardot (2001). Biostratigraphic data from Chrons C21n, C21r and C22n (~Cores 37-42) were not included due to a likely hiatus and ambiguity in polarity zone boundaries. ODP Site 1262 (Walvis Ridge) was drilled during Leg 208, and is located in the southeastern Atlantic Ocean, off the northwestern flank of Walvis Ridge (27°11.15´S, 1°34.62´E). The relative placement of bioevents within the magnetostratigraphic framework is from Agnini et al. (2007, table 1).

ODP Hole 1090B (Agulhas Ridge) was drilled during Leg 177 and is located in the southeast Atlantic sector of the Southern Ocean (42°54’S, 8°53’E). Calcareous nannofossil data for this Site are from Marino and Flores (2002a, b), with depth of polarity zones from Channell et al. (2003). Data are integrated through C18n?, where magnetostratigraphy becomes more ambiguous (Channell et al. 2003, fig. 4).

Deep Sea Drilling Program (DSDP) Site 577 was drilled during Leg 86 and is located in the northwestern Pacific Ocean (32°26.51'N; 157°43.40'E). Calcareous nannofossil data are from Monechi (1985) with magnetostratigraphic data from Bleil

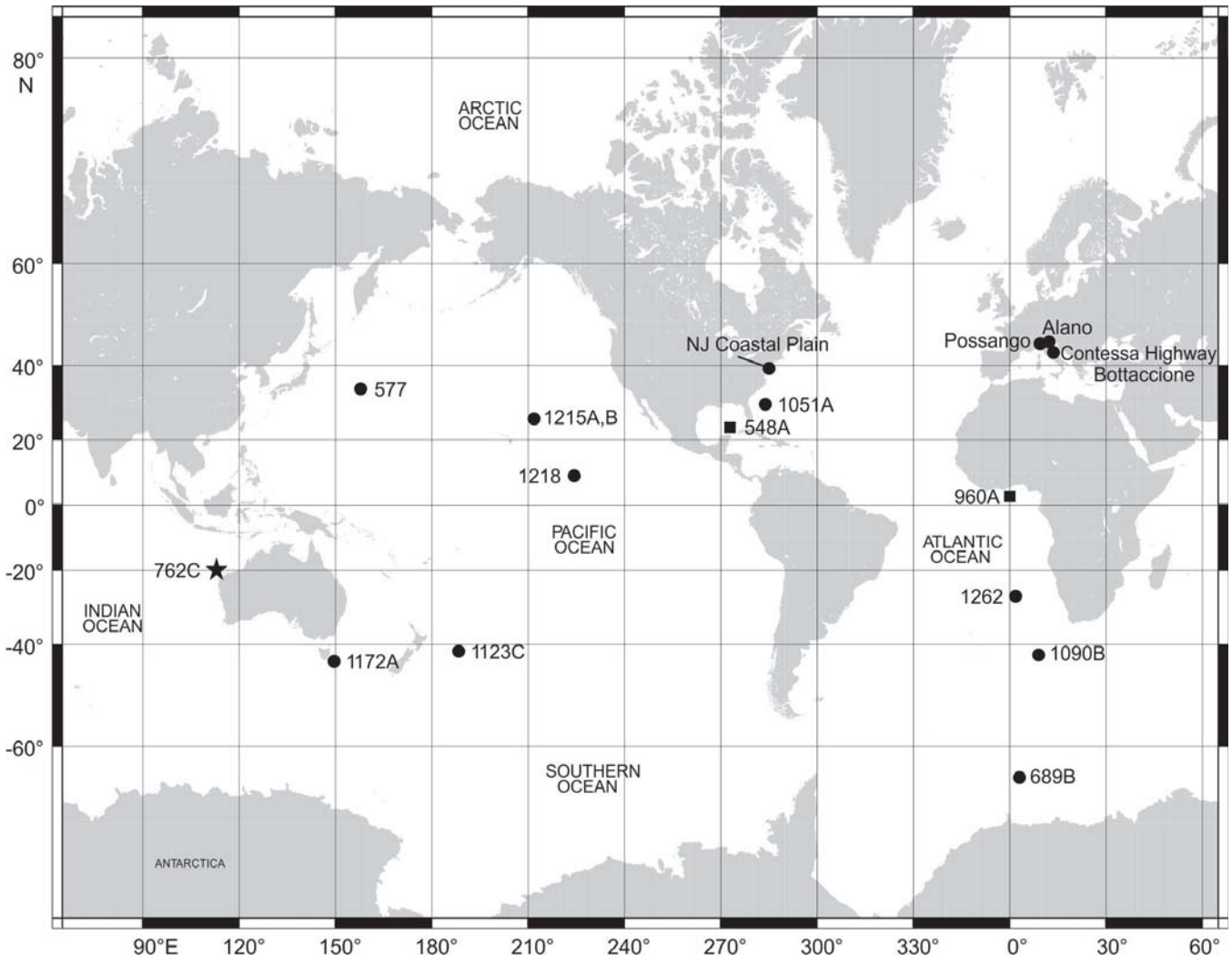

TEXT-FIGURE 1
Site Map: Global site map showing the primary locality examined in this study (Star = ODP Site 762C, NW Australian Shelf), as well as additional sites used for comparison of calcareous nannofossil biochronology. Expanded detail of Site 762 modified from Campbell Howe and Rexilius (2004).

(1985). Events are calibrated only from C24n-C25n, as depths of polarity reversals become ambiguous above this interval.

ODP Sites 1218 (8°53.378'N, 135°22.00'W) and 1215 (26°01.77'N, 147°55.99'W) were drilled during Leg 199 in the central equatorial Pacific Ocean. Magnetic reversal calibration and biostratigraphic data for Site 1218 are both from Pälike et al. (2006). Calcareous nannofossil data for Holes 1215A-B are from Raffi Backman and Pälike (2005) with depths of paleomagnetic reversals from Lyle et al. (2002).

ODP Hole 1123C (Eastern New Zealand) was drilled during Leg 181 and is located in the southwest Pacific (41° 47.147'S, 171° 29.941'W). Calcareous nannofossil data are derived from McGonigal and Di Stefano (2002) with magnetostratigraphy for Hole 1123C from the Leg 181 Shipboard Scientific Party (2000).

ODP Hole 1172A (East Tasman Plateau), located in the Southern Ocean (43°57.5854'S, 149°55.6961'E), was drilled during ODP Leg 189. Calcareous nannofossil and magnetostratigraphic data are from Wei McGonigal and Zhong (2003) and Stickley et al. (2004).

ODP Leg 113 Hole 689B (Maud Rise) is located in the eastern Weddell Sea (64°31.009'S, 3°5.996'E). Calcareous nannofossil data are from Wei and Wise (1990), with magnetostratigraphic data from Florindo and Roberts (2005).

DATA AND METHODS

Magnetostratigraphy

The magnetic polarity data for Hole 762C are from ODP Leg 122 Scientific Results, which gives detailed sampling, laboratory, and analytical procedures (Galbrun 1992). The polarity reversals and original magnetostratigraphic interpretation of Galbrun (1992) are illustrated in text-figure 2. Poor core recovery in several sections creates ambiguous magnetostratigraphic patterns and greatly limits interpretation. Though the original

interpretation does use nannofossil biostratigraphy to aid correlation of the magnetic polarity sequence, several issues exist with the original age model. Berggren et al. (1995b) noted that Hole 762C represents a well preserved and expanded Eocene section; however, despite Hole 762C's stratigraphic 'potential', data from this site was not used in the calibration of the BKSA95 IMBS (integrated magnetobiostratigraphy). The authors question the original interpretation of Galbrun (1992), noting that "the magnetobiostratigraphic correlations in the site appear to be rather ambiguous" (Berggren et al. 1995, p. 184). Despite the intermittent core recovery through Eocene sediments at Hole 762C, it is possible to generate a relatively robust age model with integration of additional stratigraphic data. The revised magnetostratigraphy for Hole 762C is discussed in the interpretation section below.

Nannofossil Biostratigraphy

The detailed biostratigraphy, assemblage data, dominance trends, and systematic paleontology for Hole 762C have been examined in Shamrock and Watkins (*this volume*), which provides information in nannofossil sample selection, preparation, and data collection. Sample interval and depth data for nannofossil biostratigraphy are provided in Appendix 1 for Cores 3-29. Core samples and smear slides are located within the collections of the ODP Micropaleontological Reference Center at the University of Nebraska State Museum (UNSM). Nannofossil data for Core 2 is from Siesser and Bralower (1992).

Biostratigraphic events will be referred to as lowest occurrence (LO), lowest consistent occurrence (LCO), highest occurrence (HO), highest consistent occurrence (HCO), acme beginning (AB), acme end (AE), abundance increase (INC) and cross-over (XO) (cross-over or dominance reversal).

Two well known biozonation schemes are widely employed in Paleogene calcareous nannofossil biostratigraphy. Data from Shamrock and Watkins (*this volume*) includes both the low-latitude CP Zonation of Okada and Bukry (1980, with select subzones and secondary markers of Perch-Nielsen 1985) and the cosmopolitan to high-latitude NP Zonation Martini (1971, with select subzones of Aubry 1991). Strict application of some zonal boundaries was not possible, due to rarity or absence of some marker taxa such as *Rhabdosphaera gladius*, *Discoaster bifax* and *Nannotetrina alata.* The Mediterranean MNP zonation (Catanzariti and Rio 1997) is, in some ways, more applicable to this study. Markers such as *Cribrocentrum reticulatum, Dicctyococcites bisectus*, *Sphenolithus obtusus*, *S. spiniger* and *S. furcatolithoides* are more abundant in Hole 762C than the *Chiasmolithus* and *Nannotetrina* spp. commonly utilized. The MNP scheme is not illustrated here as it extends only to the upper Lutetian, covering only ~1/2 of the study interval. The CP and NP nannofossil biostratigraphy at Hole 762C is illustrated in text-figure 2, and sample depths of key nannofossil marker taxa are summarized in Table 1. Concurrent application of both zonation schemes with the new data set (Shamrock and Watkins *this volume*) identifies zones and subzones that are absent from both the NP and CP zonation schemes:

1) Subzone CP8b is absent from Hole 762C, as both the primary marker (LO *Campylosphaera eodela*) and the secondary marker (LO *Rhomboaster* spp.) are concurrent with the biomarker for CP9a (LO *Discoaster diastypus*) (28-1-59cm, 412.59 mbsf). This missing subzone is linked to a hiatus associated with the PETM.

2) NP13 is marked by the HO of *Tribrachiatus orthostylus,* which is also the secondary marker for CP11 (Perch-Nielsen 1985); however, there is no apparent separation between this biohorizion and the base of NP14a (LO *Discoaster sublodoensis*), as both events were observed in the same sample. In fact, extrapolation upward and downward for the HO and LO, respectively, creates a depth cross-over as shown in Table 1. While it is quite possible that the LO of *D. sublodoensis* occurs 'early' at this locality, creating convergence, this relationship is also likely related to a hiatus within this interval.

3) CP13 is divided into subzones CP13b and CP13c by the LO and HO of *Chiasmolithus gigas*, respectively. These subzonal markers are often similarly applied to NP15. Zone NP15c is severely reduced and subzone CP13c is absent from Hole 762C. The HO of *Ch. gigas* (14-6-50, 292 mbsf) shows very little stratigraphic separation from either the base of NP 16 (HO of *Nannotetrina fulgens* (14-5-115, 291.15 mbsf) or the base of CP14 (LO of *Reticulofenestra umbilica*) (14-6-50, 292.00). The relative depths of these three bioevents strongly suggest a hiatus in this interval (Figure 2). These issues are considered when integrating various data sets, as well as in the final age model. Calcareous nannofossil tie-points used in the revised age model are summarized in Table 2.

Planktonic Foraminifera Biostratigraphy

The original planktonic foraminiferal biostratigraphy for Hole 762C (Shipboard Scientific Party 1990) was conducted at coarse sample spacing of one sample (core catch)/core, or approximately every 10m. Such resolution does not allow these bioevents to be used as calibrated tie points within the final age model; however, the planktonic foraminiferal P zonation (Berggren and Miller 1988; Berggren and Pearson 2005) as applied at Hole 762C can help to guide the correlation of a particular polarity reversal to the GPTS (geomagnetic polarity timescale). These data give significant support to the present interpretation, based primarily on higher resolution nannofossil biostratigraphy. Core-scale resolution of planktonic foraminiferal P zones is shown in text-figure 2. Specific intervals or correlations used to aide in magnetostratigraphic interpretations are discussed below.

Stable Isotope Stratigraphy

Stable isotope stratigraphy provides another valuable set of tie-points in our revised age model for Site 762, with bulk analysis of $\delta^{13}C$ and $\delta^{18}O$ from Thomas Shackleton and Hall (1992). Significant advancements have been made in Paleogene isotope stratigraphy since the time of the original publication. The development of high-resolution global $\delta^{13}C$ and $\delta^{18}O$ records allows identification of several well-calibrated excursions throughout the Eocene (Bohaty et al. 2009; Cramer et al. 2009; Sluijs et al. 2008; Jovane et al. 2007; Nicolo et al. 2007; Lourens et al. 2005; Bohaty and Zachos 2003; Cramer et al. 2003; Zachos et al. 2001; Salamy and Zachos 1999). This plethora of research has also generated multiple names for a single isotopic event, which are summarized in Sluijs et al. (2008). For brevity, only the first of the several names provided in Table 3 will be used in discussion.

Many of the paleoenvironmental events recorded globally in $\delta^{13}C$ and $\delta^{18}O$ data have been correlated to nannofossil

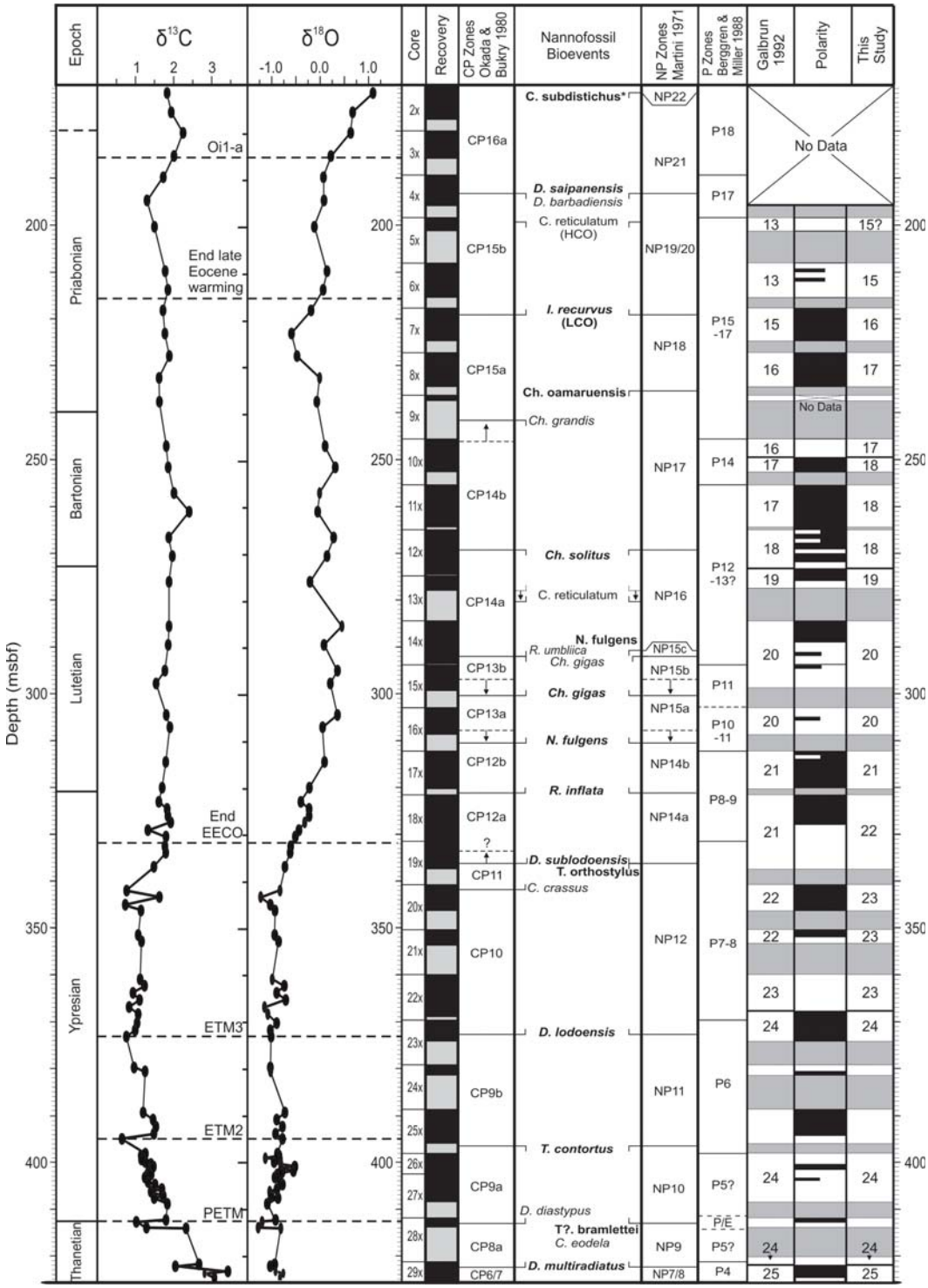

TEXT-FIGURE 2

Hole 762C Data Suite: Correlation of stratigraphic data sets from Site 762C, showing, from left to right, core depth (msbf), lithologic unit/subunit (Shipboard Scientific Party 1990), geologic stage, δC (‰), δO (‰), core number, core recovery, calcareous nannofossil CP zonation, nannofossil bioevents, nannofossil NP zonation, planktonic foraminifera P zonation, magnetostratigraphy of Galbrun (1992), magnetic polarity sequence, and present magnetostratigraphic re-interpretation. Isotopic data (δC and δO) from Thomas, et al. (1992), with interpretation of isotopic events shown as dashed lines. Chemical events correlate to Table 4 (column 1). CP biomarkers of Okada and Bukry (1980) in bold. NP biomarkers of Martini (1971), with select subzones of Aubry (1991), shown in italic. Joint markers for CP and NP zones shown in both bold and italic. Locations of CP and NP zonal boundaries reflect the midpoint between the observed event and the sample above (for HOs) or below (for LOs). Nannofossil biozone boundaries are shown by solid lines; however, dashed lines are used to show the observed event depth where sample spacing creates = 2.0 m gap around the bioevent midpoint. Sample depths for nannofossil biostratigraphy provided in Table 2. *Bioevent data from Siesser and Bralower (1992). Coring gaps are shown in grey in both core recovery and magnetic polarity columns. Magnetic polarity indicated by black (white) fill for normal (reverse) polarity. Revised magnetostratigraphy correlated to the GPTS of Ogg, et al. (2008)

biostratigraphy and magnetostratigraphy, and can provide well calibrated dates (Table 3). The dates applied to several isotopic excursions were derived by the original authors using GPTSs such as the Cande and Kent (1995, hereafter CK95). The original dates for such isotopic excursions have been recalibrated to the timescale of Ogg Ogg and Gradstein 2008. Though the sample spacing of stable isotopic data from Hole 762C was quite coarse (~2 samples/core, Cores 2-17, 28-29; ~1sample/core, Cores 18-27) (Thomas Shackleton and Hall 1992, table 1), high-resolution $\delta^{13}C$ and $\delta^{18}O$ records are available from other localities and studies (Cramer et al. 2009; Nicolo et al. 2007; Bohaty and Zachos 2003; Zachos et al. 2001, others). These additional records allow us to identify key isotopic excursions and to make relatively robust correlations, even when faced with limited data sets such as those from Hole 762C. Not all global paleoenvironmental events can be identified in the isotopic records from Hole 762C, such as some short-lived hyperthermals (Nicolo et al. 2007; Lourens et al. 2005); however, several events are identified by comparing the isotopic excursion patterns to the magnetostratigraphy and nannofossil biostratigraphy. These events, as well as the criteria used to identify them in Hole 762C, are summarized below (see also Table 3 and text-figure 2).

The age assigned to the PETM at Site 762 is derived from Cramer et al. (2003), as the Chron C25n/C24r boundary age – 0.924 myr. The depth of the ETM2 (Eocene thermal maximum 2) in Hole 762C was determined by both the magnitude of the CIE (~1.0‰, Cramer et al. 2003), and by correlation to nannofossil zone CP9b/NP11 boundary. Two dates are provided in the literature for the ETM2 event, though very closely spaced (Table 3). The upper date is derived by determining the relative placement of the Elmo horizon (Lourens et al. 2005) within Chron C24r at Site 1262 (~115.5-153.5 mcd) (Bowels 2006), then converting that relative placement to the Ogg Ogg and Gradstein 2008 GPTS. This retains the relative placement of this excursion by Lourens et al. (2005) below the Chron C24r/C24n polarity reversal. The lower ETM2 date is derived from Cramer et al. (2003), placed between the Chron C24r/C24n reversal and the base of NP11. We identify the ETM2 excursion below the Chron C24r/C24n reversal in Hole 762C, so apply the date provided by Lourens et al. (2005). The ETM3 was originally described as the "X" event by Röhl et al. (2005), and is correlated to foraminiferal zone P7 and nannofossil zone CP10. Both Agnini et al. (2007) and Galeotti et al. (2010) identify the ETM3 event in Chron C24n.1n (52.65-53.00 Ma) at the Contessa Highway section. The date we apply to the EMT3 in Hole 762C (Table 3) is based on those correlations to Chron C24n.1n, as well as the association by Galeotti et al. (2010) of the ETM3 with the LO of *Discoater lodoensis* Bramlette and Riedel 1954 within Chron C24n.2r (53.23 Ma 2008 GPTS; 52.85 Ma, BKSA95), also observed in Hole 762C.

A significant warming trend occurred from the late Paleocene through the early Eocene. This global warmth peaked with the EECO (Early Eocene Climatic Optimum), ending at ~49.8 Ma (Chron C22r) (Bohaty and Zachos 2003). Delineating the termination of a long term trend can be difficult, with much greater stratigraphic freedom than the short-lived hyperthermals discussed above. Placement of the EECO in Hole 762C is guided by recent isotopic curves of Cramer et al. (2009), who identified the end of the EECO just past the peak negative $\delta^{18}O$ excursion, on the falling limb of the curve. The age applied to the end of the Late Eocene warming in Hole 762C was derived from Vonhof et al. (2000), who dates the base of the "Vonhof" cooling event (Bohaty and Zachos 2003) at 35.5 Ma ($^{40}Ar/^{39}Ar$), correlating to nannofossil zones CP15/NP18. Global isotopic trends from Bohaty and Zachos (2003, fig. 2) show a direct transition from the late Eocene warming trend into the "Vonhof" cooling event, and we adopt a similar convention in Hole 762C (Table 3, text-figure 2).

REVISED MAGNETOSTRTIGRPHY

Despite the presence of a thick and expanded Eocene section at Site 762, intermittent core recovery (and several hiatuses) impedes direct correlation between the polarity reversals observed and the idealized polarity pattern the GPTS. The original magnetostratigraphy of Galbrun (1992) used the nannofossil biostratigraphy of Siesser and Bralower (1992); however, here we present a re-interpreted magnetostratigraphy for the Eocene section of Hole 762C, facilitated by the integration of a revised calcareous nannofossil biostratigraphy (Table 1), as well as planktonic foraminifera, and isotopic data, calibrated to the GPTS of Ogg Ogg and Gradstein (2008).

The correlations among calcareous nannofossils, planktonic foraminifera, $\delta^{13}C$ and $\delta^{18}O$ isotopic excursions, and magnetic polarity reversals observed at Site 762 are summarized in text-figure 2. The polarity reversal pattern (center) is shown against the original magnetostratigraphic interpretation of Galbrun (1992) (left), in comparison to the revised interpretation of this study (right). Sample intervals for magnetic polarity data are provided in Galbrun (1992, appendix 2). Primary evidence used in the interpretation of each magnetochron is discussed below. These revisions allow adjustment of magnetostratigraphic tie-points, with these reversals integrated into the revised age model (Table 4).

Polarity zones and GPTS Chron designations are discussed by core and illustrated in text-figure 2. The re-interpretation was relatively straight-forward through the Ypresian and Priabonian, but became increasingly difficult in the Lutetian and Bartonian. This is related to both the quality and quantity of stratigraphic data at various intervals, as well as ambiguity through intervals with poor core recovery and/or stratigraphic hiatuses. This portion of the section was constrained as much as possible by all available data, as well as confidence in the re-interpretations above and below.

Cores 3-4: No magnetostrtigraphic data or interpretation is provided by Galbrun (1992) above Core 5; however, a number of biostratigraphic and isotopic datums are observed in this interval suggesting that this interval is best correlated to Chron C13r. The HOs of *Discoaster saipanensis* and *D. barbadiensis* is observed in Core 4 (Table 2), and the *Clausicoccus* spp. acme base is observed in Core 3. In addition, Pearson et al. (2008) correlated the first step of Oi-1 to Chron C13r, and these significant positive isotopic shifts are seen in Core 3 at Hole 762C (text-figure 2). This extrapolation of Cores 3-4 to Chron 13r is necessary to interpret Cores 5-6.

Core 5-6

Though attributed to Chron C13r by Galbrun (1992), this interval is now identified as C15r. This interpretation is due to both the extrapolated correlation of Cores 3-4 to Chron 13r, as well as several lines of evidence that support correlation of Cores 5-6

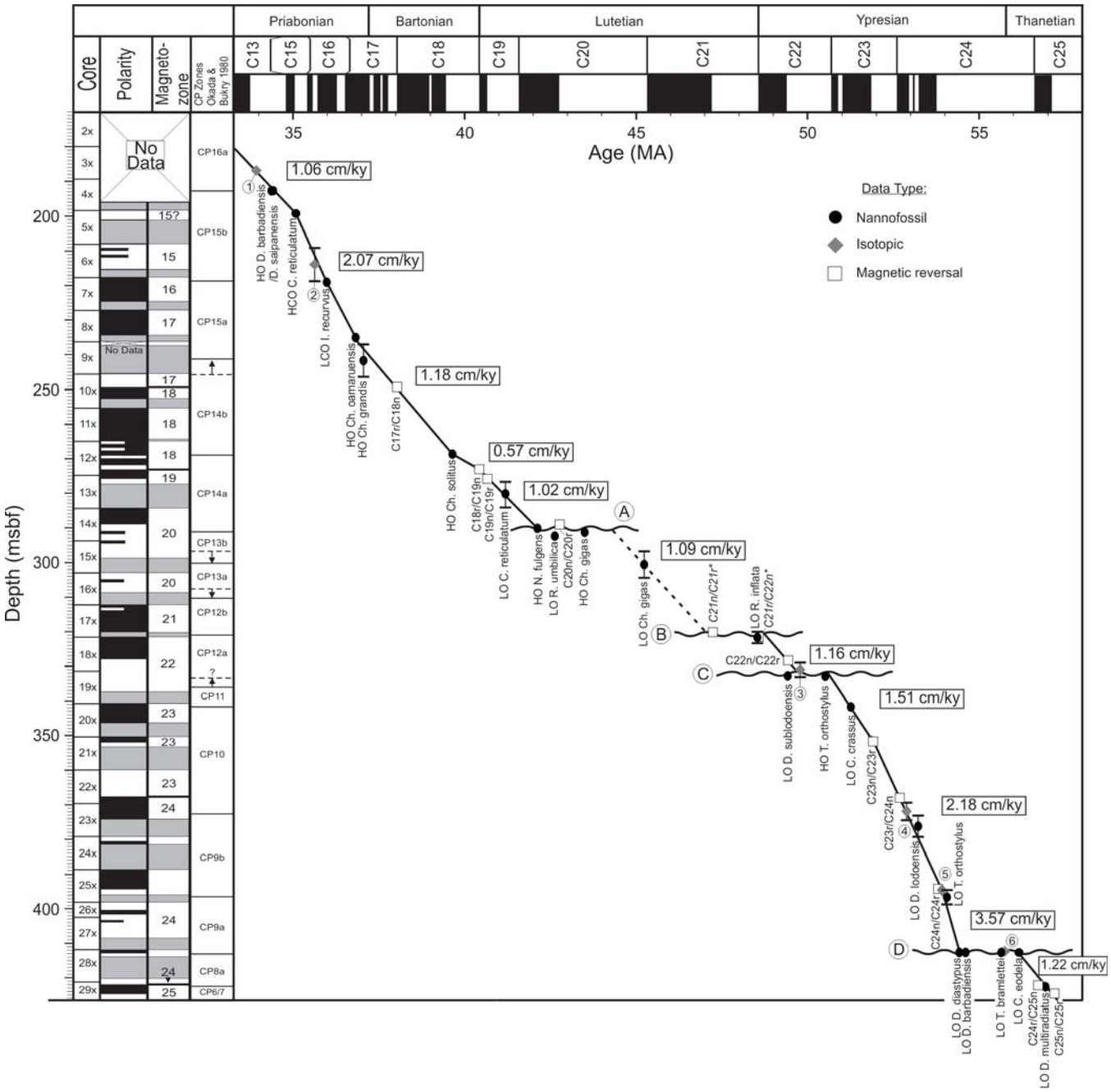

TEXT-FIGURE 3
Age-Depth Model: Age-depth model and derived sediment accumulation rates for ODP Site 762C, correlated to the GPTS of Ogg, et al. (2008) and Eocene stages (horizontal axis). Along vertical axis (from left): depth (msbf), core number, magnetic polarity, revised magnetostratigraphy, and nannofossil biostratigraphy. Stratigraphic model derived using calcareous nannofossil, isotopic, and magnetostratigraphic data (Tables 3-5, respectively). Events and depths are shown as sample midpoints. Vertical bars around data points show potential depth errors around widely spaced samples. Accumulation rates are calculated between tie-points, assuming constant sedimentation. Where the section is interrupted by a disconformity, sedimentation rates of adjacent sections were used to extrapolate the upper and lower ages and estimate the duration of the hiatus. Circled letters correspond to hiatuses as discussed in text. Three hiatuses (A, C, D) were identified primarily with nannofossil data. Hiatus B was inferred using magnetic polarity and sedimentation rates (See text for further discussion). The large sample gaps around the LO of *Ch. gigas* gives much latitude in interpretation of the sedimentation rate, as indicated by the dashed line (See text for further discussion).

TABLE 1
Nannofossil Biostratigraphy: Summary of revised nannofossil biostratigraphy of Site 762C from Shamrock and Watkins (2012). Standard CP Zonation of Okada and Bukry (1980) at left. NP zonation of Martini (1971) with select subzones of Aubry (1991) at right. Midpoints were extrapolated using the sample above (for LOs) or below (for FOs).

CP Zonation							NP Zonation					
Zone		Event	Marker Taxa	Sample Int.	Depth	Midpt.	Zone	Event	Marker Taxa	Sample Int.	Depth	Midpt.
16	a	HO	D. saipanensis D. barbadiensis	4-3-100/4-3-50	192.50-193.00	192.75	21	HO	D. saipanensis	4-3-100/4-3-50	192.50-193.00	192.75
15	b	LO	I. recurvus	7-1-50/7-2-125	218.00-220.25	219.13	19/20	LO	I. recurvus	7-1-50/7-2-125	218.00-220.25	219.13
	a	HO	Ch. grandis	10-1-50/9-1-46	236.96-246.50	241.73	18	LO	Ch. oamaruensis	8-5-50/9-1-46	233.50-236.96	235.23
14	b	HO	C. solitus	12-3-125/12-3-50	268.50-269.25	268.88	17	HO	Ch. solitus	12-3-125/12-3-50	268.50-269.25	268.88
	a	LO	R. umbilica	14-6-50/14-6-147	292.00-292.97	292.49	16	HO	N. fulgens	14-5-115/14-5-50	290.50-291.15	290.83
13	c	HO	Ch. gigas	14-6-50/14-5-115	291.15-292.00	291.58	15	c	HO	Ch. gigas	14-6-50/14-5-115	291.15-292.00	291.58
	b	LO	Ch. gigas	15-3-48/16-1-48	296.98-303.48	300.23		b	LO	Ch. gigas	15-3-48/16-1-48	296.98-303.48	300.23
	a	LO	N. fulgens	16-4-45/17-1-51	307.95-313.01	310.48		a	LO	N. fulgens	16-4-45/17-1-51	307.95-313.01	310.48
12	b	LO	R. inflata	17-5-148/18-1-50	319.98-322.50	321.24	14	b	LO	R. inflata	17-5-148/18-1-50	319.98-322.50	321.24
	a	LO	D. sublodoensis	19-2-52/19-2-125	333.52-334.25	333.89		a	LO	D. sublodoensis	19-2-52/19-2-125	333.52-334.25	333.89
11		LO	C. crassus	20-1-50/20-1-125	341.50-342.25	341.88	13		HO	T. orthostylus	19-2-52/19-1-125	332.75-333.52	333.14
10		LO	D. lodoensis	24-1-54/23-3-54	373.01-379.54	376.28	12		LO	D. lododensis	24-1-54/23-3-54	373.01-379.54	376.28
9	b	HO	T. contortus	26-1-49/25-5-43	394.93-398.30	396.62	11		HO	T. contortus	26-1-49/25-5-43	394.93-398.30	396.62
	a	LO	D.diastypus	28-1-59/28-1-125	412.59-413.25	412.92	10		LO	T?. bramlettii	28-1-59/28-1-126	412.59-413.25	412.92
8	b	LO	C. eodela Rhomboaster spp.	28-1-59/28-1-126	412.59-413.25	412.92	9		LO	D. multiradiatus	29-1-50	422.00	422.00
	a	LO	D. multiradiatus	29-1-50	422.00	422.00							

to Chron C15r, including the HCO of *Cribrocentrum (Reticulofenestra) reticulatum* in Core 5 (HO = Core 4) and the HO of planktonic foraminifera *Turborotalia pomeroli* within sample 762C- 5x-CC.

Core 7

Correlated to Chron C15n in Galbrun (1992), this section is re-interpreted as Chron C16n, based on the LO of *Isthmolithus recurvus* (Table 2). This adjustment also brings the LO of *Reticulofenestra oamaruensis* into better agreement with its calibration to Chron C16n. Though the event is still observed slightly above Chron C16n, this may be due to the mid-latitude paleogeography of Site 762. In addition, a notable period of Late Eocene warming terminates with the "Vonhof" cooling event (Zachos et al. 2001; Vonhof et al. 2000), calibrated to Chron C16n, identified as a $\delta^{18}O$ isotope shift within Core 762C-7 (text-figure 2, Table 3).

Core 8

Originally attributed to Chron C16n, this study finds greater stratigraphic agreement with assignment to Chron C17n, due to the HOs of both *Chiasmolithus grandis* and *Ch. oamaruensis* (Table 2). The early 'spike' of *Isthmolithus recurvus*, correlated to C17n by Fornaciari et al. (2010) and Agnini et al. (2011) is also identified in this interval in Hole 762C.

Core 10

The temporary hiatus of *Sphenolithus predistentus* is observed in Core 10, correlated to C18n by Fornaciari et al. (2010). In addition, core 10 has been correlated to planktonic foraminiferal zone P14, which is limited to Chron C18. Though this designation comes only from sample 762C-10x-CC, it indicates that at least some of this core must belong to Chron C18, suggesting that the polarity reversal captured in this section is the Chron C18n/17r boundary (text-figure 2).

Core 11

This normal polarity zone is attributed to Chron C18 based on the HO of *Sphenolithus spiniger* (Fornaciari et al. 2010), as well as the presence of Chron C18, above, and Chron C18 and C19, below.

Core 12-13

This interval retains the original interpretation of Galbrun (1992). The HO of *Chiasmolithus solitus*, correlated to Chron C18, occurs within Core 12, as well as the LCO of *C.*

reticulatum in Chron C19 (Table 2). Core 12 contains a problematic series of thin magnetic reversals that are difficult to interpret. These may be due to overprinting of the original magnetic signal, or may represent a condensed section, as derived sedimentation rates drop considerably, being the only interval with rates < 1.0cm/ky.

Core 14-16

As in Galbrun (1992), we attribute this interval to Chron C20. This designation is supported by several bioevents, including the LO of *Ch. gigas,* HO of *Ch. gigas*, HO of *N. fulgens,* planktonic foraminiferal zone P11, and the HO of planktonic foraminifera *Morozovella aragonensis*, all correlate to Chron C20r.

Core 17

This interval is attributed to Chron C21, based on the calibration of LO of *Rhabdosphaera (Blackites) inflata* to Chron C21r in the BKSA95, as well as observation in Chron C21n at both Bottaccione (Monechi and Thierstein 1985) and at ODP Site 1051 (Table 5). Assignment of Core 17 to Chron C21 is also supported by the LO of *N. fulgens*, calibrated to Chron 21n (BKSA95) (text-figure 2)

Core 18-19

Attributed to Chron C21 by Galbrun (1992), this section is now correlated to Chron C22. The *Discoaster* spp. AE is observed in this interval, correlated to Chron C22r by Agnini et al. (2006). Core 19 also contains significant positive isotopic shifts: $\delta^{13}C$ increases by 0.71‰ (341.82-336.72 msbf) while $\delta^{18}O$ increases by 0.5‰ (343.21-336.72 msbf) toward a sustained low through the Lutetian (text-figure 2). This shift likely represents the end of the EECO, also calibrated to Chron C22r (Bohaty and Zachos 2003).

Core 20-22

The authors agree with Galbrun (1992) with correlation of Core 22 to Chron C23r; however, the original interpretation of Cores 20-21 to Chron C22 is amended in this study to also correlate to Chron C23 (text-figure 2). The LO of *Coccolithus crassus*, reported from Chron C23n from several European sections (Table 5), is observed in this interval (text-figure 2, Table 2). The *Discoaster* spp. AB at Site 762, discussed in Shamrock and Watkins (*this volume*) is correlated to Chron C23n by Agnini et al. (2006). This reinterpretation is also supported by planktonic foraminiferal data, with the co-occurrence of *Morozovella formosa* and *M. aragonensis* limited to Chron C23n.

Core 22-25

The present analysis agrees with Galbrun (1992) with correlation to Chron C24n. This interpretation is supported by nannofossil data (LO *Discoaster lodoensis*, LO *Girgisia gammation*, planktonic foraminifera data (absence of *Morozovella aragonensis*, with LO in Chron C23r, above) and $\delta^{13}C$ isotopic data (ETM3) (text-figure 2).

Core 25-28

The present interpretation is in agreement with Galbrun (1992) with correlation to Chron C24r. Supporting data include several bioevents calibrated to this magnetochron in the BKSA95 (Table 5), such as the LOs of *D. diastypus, D. barbadiensis,*

TABLE 2
Nannofossil Tie-points: depth ranges and midpoints of calcareous nannofossil data integrated into the revised age model. Nannofossil ages represent calibrated dates from BKSA95, converted to the 2008 GPTS of Ogg, et al., unless otherwise indicated. *Age for LO *C. crassus* derived from Bottaccione, Possagno, and Contessa Highway sections (Table 6). **Age for the LO *D. diastypus* from averaging calibrated dates from Site 1262, Site 1215A, and Site 577. †Age for LO *D. barbadiensis* from averaging calibrated dates from Site 577 and the Bottaccione and Contessa Highway sections (Italy). ††This depth represents the deepest sample examined in Shamrock and Watkins (2012) but also correspond to the midpoint depth of Siesser and Bralower (1992), who sampled much deeper in the core.

Event	Taxa	Top-Base (msbf)	Midpoint	Age (MA)
HO	*D. saipanensis*	192.50-193.00	192.75	34.35
HO	*D barbadiensis*	192.50-193.00	192.75	34.45
HCO	*C. reticulatum*	199.00-199.75	199.38	35.09
LCO	*I. recurvus*	218.00-220.25	219.13	35.98
HO	*Ch. oamaruensis*	233.50-236.96	235.23	36.83
HO	*Ch. grandis*	236.96-246.50	241.73	36.92
HO	*Ch. solitus*	268.50-269.25	268.88	39.69
LO	*C. reticulatum*	276.71-284.05	280.38	41.10
HO	*N. fulgens*	290.50-291.15	290.83	42.12
LO	*R. umbilica*	292.00-292.97	292.49	42.69
HO	*Ch. gigas*	291.15-292.00	291.58	43.51
LO	*Ch. gigas*	296.98-303.48	300.23	45.18
LO	*R. inflata*	319.98-322.50	321.24	47.95
HO	*T. orthostylus*	332.75-333.52	333.14	50.51
LO	*D. sublodoensis*	333.52-334.25	333.89	49.41
LO*	*C. crassus*	341.50-342.25	341.88	51.26
LO	*D. lodoensis*	373.01-379.54	376.28	53.23
LO	*T. orthostylus*	394.93-398.3	396.62	54.14
LO**	*D. diastypus*	412.59-413.25	412.92	54.42
LO†	*D. barbadiensis*	412.59-413.25	412.92	54.61
LO	*T. bramlettei*	412.59-413.25	412.92	55.65
LO	*C. eodela*	412.59-413.25	412.92	56.21
LO	*D. multiradiatus*		422.00††	56.98

Tribrachiatus bramlettei, T. contortus and *T. orthostylus*; the HOs of *Fasciculithus* spp., *T. contortus*; planktonic foraminiferal zone P5, as well as isotopic excursions that have been tied to Chron C24r (PETM and ETM2) (Table 3).

Core 29

As reported in Galbrun (1992), the upper polarity reversal captured in Core 29 is identified as the Chron C25n/C24r reversal boundary, with the lower correlated to the Chron C25r/C25n reversal. This interpretation is supported by the presence of *Discoaster nobilis*, the HO of *Ericsonia robusta*, the LO of *D. multiradiatus* and planktonic foraminiferal zone P4.

TABLE 3
Isotopic Tie-points: depth ranges and midpoints of δC and δO isotopic excursion events integrated into the revised age model. Magnetochron correlations from primary references (right). Dates originally given in the CK95 or BKSA95 timescales were converted to the GPTS of Ogg, et al. (2008).

Chemical Event	Midpoint (msbf)	Age 2008 GPTS, Ogg et al	Age CK95/BKSA95	Chron	Source
Oi-1, Step 1	187.00	33.93	33.75	C13r	Pearson et al. 2008
End Late Eocene warming / "Vonhof" cooling event	213.30	35.5	35.5	C16n.1n	Vonhof et al. 2000 Zachos et al. 2001
End EECO	331.22	49.78	49.00	C22r	Bohaty & Zachos 2003
ETM3/"X" event/Event "K"	372.35	52.88		C24n.1n	Galeotti et al. 2010
ETM2/H1/ELMO	394.85	53.91	53.44	C24r	Lourens et al. 2005
		53.81-54.09	53.35-53.61	C24n	Cramer et al. 2003
PETM	412.65	55.74	54.98	C24r	Cramer et al. 2003

We demonstrate that the reinterpreted magnetostratigraphy at Hole 762C gives well defined intervals through the Eocene that compare well with the idealized magnetostratigraphy of published GPTSs (Ogg Ogg and Gradstein 2008; Gradstein Ogg and Smith 2004; Cande and Kent 1995), except where hiatuses have been identified, and in the lower Bartonian (Core 12) where magnetic reversal patterns are ambiguous. Micropaleontological data lends high confidence to the magnetostratigraphic interpretation of Cores 5-29 at Site 762; however, poor core recovery, sparse data points and ambiguous polarity reversals decrease confidence within some problem intervals.

AGE-DEPTH PLOT

Biostratigraphic, isotopic, and magnetostratigraphic data, correlated to the Ogg Ogg and Gradstein 2008 GPTS, are integrated to construct a revised age-depth plot for Hole 762C (text-figure 3). Dates of nannofossil bioevents are from BSKA95, recalibrated to Ogg Ogg and Gradstein 2008. Constant sedimentation was assumed between age calibration points. A summary of the primary biostratigraphic, isotopic and magnetostratigraphic tie-points shown in text-figure 3 is provided in Tables 3-5, respectively.

Stratigraphic Hiatuses

Integration of biostratigraphy, magnetostratigraphy, and $\delta^{13}C$ and $\delta^{18}O$ data from Hole 762C has demonstrated the presence of a least four previously unidentified Eocene hiatuses, illustrated in text-figure 3 and summarized in Table 6. These are treated separately, below:

Hiatus A: the shallowest hiatus is identified at 289.75 msbf, at the midpoint between the HO of *N. fulgens* (Table 2) and the Chron C20n/C20r reversal (Table 4). This hiatus also includes the LO of *R. umbilica* and the HO of *Ch. gigas* (text-figure 3). This disconformity includes nannofossil zone CP13c/NP15c and portions of both Chron C20n and Chron C20r. The upper and lower age limits for this hiatus are dated to 42.02 and 44.22 Ma, respectively, a duration of ~2.2 myr.

Hiatus B: three of the four hiatuses discussed in this section are readily identified with nannofossil biostratigraphy; however, this additional hiatus was identified based on the relationships between magnetic reversals and sedimentation rate. The normal polarity interval in Core 18 has been attributed to Chron C22, based on the HO of *T. orthostylus* (Table 2), the *Discoaster* spp. AE (Table 5), and isotopic shifts indicating the end of the EECO (Table 3); however, the normal polarity interval in Core 17 has been attributed to Chron C21, based on the LO of *R. inflata* (Tables 3, 6). This interpretation implies that the reverse polarity interval of Chron C21 must occur in the ~1.75m coring gap at the base of Core 17 (text-figures 2, 3). Sedimentation rates must slow significantly to ~0.13cm/ky to fit a 1.37 myr polarity reversal within this coring gap. All derived sedimentation rates through the Eocene at Hole 762C are > 1.0cm/ky (less Core 18), suggesting a hiatus between these two normal polarity intervals. As all of Chron C21r (47.23-48.60 Ma) is absent, we can first estimate a minimum duration for this hiatus of 1.37 myr. This hiatus is placed within the age model (text-figure 3) by assuming a minimum duration and assigning top and base dates of Chron 21r to the upper and lower depths of the coring gap, respectively (Table 4). The depth of the disconformity was placed at the mid-point between these two events (321.13 msbf), but also includes the LO of *R. inflata* (text-figure 3). The upper and lower age limits for this hiatus are dated to 47.10 Ma and 48.83 Ma, respectively, a duration of ~1.7 myr.

Hiatus C: the third disconformity is identified at 332.18 msbf, at the midpoint between the HO of *T. orthostylus* (Table 2) and the end of the EECO (Table 3, text-figure 2). The upper and lower age limits of this hiatus are dated to 49.79 and 50.71 Ma, respectively (~0.9 myr) and includes a portion of Chron C22r. This interval also includes the LO of *D. sublodoensis*, discussed further below.

Hiatus D: the deepest disconformity is identified at 412.78 msbf, at the midpoint between the PETM (Table 3) and a key nannofossil sample interval, containing the LOs of *D. diastypus*, *D. barbadiensis*, *C. eodela*, and *T. bramlettei* (Table 2), as well as the HO of *Fasciculithus* spp. and the LO of *T. contortus* (Table 5). This hiatus includes nannofossil zone CP8a and portions of Chron C24r. The upper and lower age limits of this hiatus are dated to 54.41 and 56.22 Ma, respectively, a duration of ~1.8 myr.

Sedimentation rates and nannofossil calibration

Identification of the stratigraphic hiatuses, totaling ~6.6 myr in duration, allows recalculation of sedimentation rates through the Eocene (text-figure 3). For simplicity, the calculated sedimentation rates do not take into account post-depositional com-

TABLE 4
Magnetic Reversal Tie-points: depth ranges and midpoints for magnetic polarity reversal boundaries integrated into the revised age model. Magnetochron reversal dates of Ogg, et al. (2008) and Cande and Kent (1995).

Chron Base	Top-Base (msbf)	Midpoint (msbf)	Age[1] (MA)	Age[2] (MA)
C17r/C18n	248.80-249.41	249.11	38.03	38.43
C18r/C19n	273.11-273.80	273.46	40.44	41.26
C19n/C19r	275.81-276.20	276.01	40.67	41.52
C20n/C20r	288.32-289.00	288.66	42.77	43.79
C21n/C21r*		320.25	47.23	47.91
C21r/C22n*		322.00	48.60	49.03
C22n/C22r	327.60-328.50	328.05	49.43	49.71
C23n/C23r	351.57-352.22	351.90	51.90	51.74
C23r/C24n	367.77-368.31	368.04	52.65	52.36
C24n/C24r	394.40-394.76	394.58	53.81	53.35
C24r/C25n	421.98-422.94	422.46	56.66	55.9
C25n/C25r	424.09-424.80	424.45	57.18	56.39

paction of the sediment; however, since the general lithology is consistent, differential compaction is not considered to greatly affected rates at various intervals. These rates are then used to derive the ages of calcareous nannofossil bioevents at Hole 762C, using the relative placement of the bioevent within a particular magnetochron. Precision decreases with lower core recovery. Error reflects only the stratigraphic resolution around nannofossil sample midpoints, and does not account for error around magnetic polarity reversals. Extrapolated dates for nannofossil bioevents at Site 762 are provided in Table 5.

Revised sedimentation rates were used to calculate a weighted average for each stage during periods of deposition. As anticipated, the highest average rates are observed in the Ypresian (~2.0cm/ky), as this period of global warmth is linked to high rates of productivity. Average sedimentation rates drop considerably in the Lutetian and Bartonian, both to ~1.1cm/ky, respectively. A partial recovery in sedimentation rates is observed in the Priabonian, increasing to ~1.6cm/ky. Though slightly elevated during the Ypresian and reduced in the middle Eocene, sedimentation rates at Site 762 are fairly consistent, with an average of ~1-2cm/ky through most of the Eocene.

The sedimentation rate between hiatuses A and B is shown as a dashed line, representing uncertainty in this calculation, due to the general lack of tie-points, significant error around existing tie-points, and truncation above and below by hiatuses (text-figure 3). The rate shown is chosen for its placement just after the Chron C21n/C21r polarity reversal (See hiatus B, above), and is well centered on the only available tie-point within this interval, despite its large sample error. In addition, this rate of > 1.0cm/ky is in good agreement with the general sedimentation trends observed at Hole 762Cs through intervals with greater tie-point control.

COMPARISON TO THE BKSA95 AND AUXILIARY SITES

Several additional Eocene sections (text-figure 1) have been included in this study for comparison of nannofossil bioevents to Hole 762C, as well as the BKSA95 (Table 5). Several studies provide event dates derived directly from the authors' age model (ODP Sites 1262, 1218, 1215, 1172, 1123, Alano and Possagno), which were recalculated from the original GPTS (geomagnetic polarity time scale) used in each study to that of Ogg Ogg and Gradstein (2008). Other localities (Bottaccione, Contessa Highway, NJ coastal plain, ODP Sites 1090, 1051, 689, and DSDP Site 577) provided no original age estimates for bioevents. Ages at these localities were instead derived by the relative position of the bioevents within a particular magnetostratigraphic chron.

Several of these studies identify the actual sample depth in which particular bioevents were observed; however, the ages of events provided in this study have been derived using the midpoint between the event depth and the sample above (for HOs) or below (for LOs). In some instances, due to the relationship between sample spacing and depths of magnetic reversals, the strict use of the midpoint shifts the bioevent into a different polarity zone. By comparison to additional studies we determined the polarity zone in which this event most likely occurs, and extrapolate the midpoint using the depth of that magnetic reversal.

All events have been recalibrated to the GPTS of Ogg Ogg and Gradstein (2008) and are directly comparable. Many studies included in Table 5 are conducted at fairly high resolution. We provide the mean age for events where the total error provided by the original author was = 0.01 Ma, so that 56.64-56.65 Ma = 56.645 Ma. Though most nannofossil bioevents at Site 762 were found to be in close correlation with the BKSA95, six such events show considerable divergence from this IMBS and/or the additional sites shown in Table 5. These bioevents are treated separately, below.

The HO of *Sphenolithus radians*: Though no date for this bioevent is provided in the BKSA95, dates have been derived from the Bottaccione and Contessa Highway Sections (Table 5). The date derived from Hole 762C is considerably younger (~34.4 Ma) than these Italian sections (38.74 and 39.65 Ma, respectively); however, the range pattern observed at Exmouth Plateau is in good agreement with that shown by Perch-Nielsen (1985, fig. 69), with consistent observation through CP14a/NP16, becoming more rare and sporadic through CP15b/NP19/20.

TABLE 5
Derived Nannofossil Dates: summary of derived ages for nannofossil bioevents at Site 762C based on the revised age model, compared to the BSKA95 and several additional, globally distributed sites. Midpoints for Site 762C are extrapolated using sample list in Table 1. Published and extrapolated ages of calcareous nannofossil bioevents are recalibrated to the GPTS of Ogg, et al. (2008). LO = lowest occurrence; LCO = lowest common occurrence;

Event	Taxa	Site 762C		BKSA95		Alano		Site 1218		Site 1172A	
		Mag	Date	Mag	Date	Mag	Date	Mag	Date	Mag	Date
AB	Clausicoccus spp.		33.91±21								
HO	D. saipanensis	C13r	34.47±03	C13r	34.35			C13r	34.41		
HO	D.barbadiensis	C13r	34.47±03	C13r	34.45			C13r	34.60		
LO	R. oamaruensis	13r	34.40±03	16n.1n	35.45						
LCO	I. recurvus	C16n.2n	36.04±06								
LO	I. recurvus	C16r	36.37±12	C16n.2n	35.98	17n.1n	37.12				
HO	C. reticulatum	C13r	34.20±02	C15r	35.09						
HCO	C. reticulatum	C15r	35.09								
HO	N. dubius	C17n.2n	37.39±40							C16r	36.37
LO	Ch. oamaruensis	C17n.1n	36.83±20	C17n.1n	36.83	C17n2n	37.54 (LRO)			C18n	38.28
HO	Ch. grandis	C17n.2n	37.39±41	C17n.1n	36.92	C17n2n	37.44±03	C17n.2n	37.54		
HO	S. spiniger	C18n.1n	38.65±06*			C18n2n	39.04±03				
HO	S. radians	C13r	34.41±04								
LO	S. predistentus	C18n.2n	39.11±06			C18r	40.03±02				
LCO	D. bisecta	C18n.2n	39.46±06			C18r	39.86±01				
LO	D. bisecta	C18r	39.96±13	C17n.3n	37.68			C18n.1n	39.46	C18n	38.50
HO	Ch. expansus	C18r	39.86±07								
HO	Ch.solitus	C18r	39.71±03	C18r	39.69	18n1n	38.14±04	C18r	39.69		
LO	C. reticulatum	C19r	41.10±36	C19r	41.10	C18r LCO	40.32			C18r	39.46
LO	R. umblilca	C20n	UNC A	C20n	42.69						
HO	Ch. gigas	C20r	UNC A	C20r	43.51						
HO	N. fulgens	C20n	42.12±03	C20n	42.12	Possagno				NJ Coastal Plain	
LO	Ch. gigas	C20r	45.18±30	C20r	45.18						
LO	S. furcatolithoides	C20r	45.18±02			Mag	Date			Mag	Date
LO	D.saipanensis	C21n	46.12±23								
LO	N. fulgens	C21n	46.12±23	C21n	46.54	C21n	45.96±01			C21n	46.27
LO	Nannotetrina spp.	C21n	47.06±16			C21r	47.33±01				
LO	R. inflata	C21r	UNC B	C21r	47.95						
HO	C.crassus	C22n	49.10±06								
HO	D. lodoensis	C22n	48.87±10			C21r	47.78±06				
HO	D. kuepperi	C21n	46.83±11								
AE	Discoaster spp.	C22r	49.93±20			C22r	50.58±03				
AB	Dict/Reticulo gp.	C22r	49.93±20			C22r	50.58±03				
HO	Toweius spp.	C22r	49.93±20*			C23n	5175±03				
LO	D. sublodoensis	C22r	50.51±03	C22n	49.41	C22n	49.13±02			C21r	48.56
HO	T. orthostylus	C22r	50.71±10	C22r	50.51	C22r	50.58±03			C23n	50.73
LO	C. crassus	C23n.2n	5124±03			C23n	50.91±03	Site 1215A, B		Site 577	
AB	Discoaster spp.	C23n.2n	5146±05			C23n	5175±03				
HO	D. diastypus	C23n	5179±03					Mag	Date	Mag	Date
LO	N. dubius	C24n.2r	53.22±01								
LCO	D. lodoensis	C24n.2r	53.22±01			C24n.1r	53.06±06	C23r	52.03±19		
LO	D. lodoensis	C24n.3n	53.39±10	C24n.2r	53.23	C24n.3n	53.65±06				
LCO	Chiphrag. spp.	C24n.3n	53.39±10								
HO	C. eodela	C24n.3n	53.39±10								
LO	G. gammation	C24n.3n	53.49±01			C24n.3n	53.44±06			C24n	52.85
HO	D.multiradiatus	C24n.3n	53.61±13					C24r-24n	54.46±51	C24n	53.41
HO	T. eminens	C24n.3n	53.69±13								
LO	D. kuepperii	C24n.3n	53.77±02							C24r	53.90
HCO	T. eminens	C24r	53.86±03								
HO	T. contortus	C24r	53.96±05	C24r	54.10	C24r	54.34±08	C24r	53.885		
LO	S. radians	C24r	53.95±06			C24r	54.34±08	C24r	54.46±51	C24r	53.90
LO	S. editus	C24r	54.05±02								
LO	T. orthostylus	C24r	53.96±07	C24r	54.14	C24r	54.34±08	C24r	53.915	C24r	53.90
HO	T. bramelttei	C24r	54.02±01	C24r	54.42	C24r	54.94±08	C24r	54.045		
LO	D. diastypus	C24r	54.42±03			C24r	55.39±08	C24r	54.31±07	C24r	54.29; **54.97**
LO	T. contortus	C24r	UNC D	C24r		C24r	55.24±08	C24r	54.375		
LO	D.barbadiensis	C24r	UNC D							C24r	54.29
HO	Fasiculithus spp.	C24r	UNC D			C24r	56.21±30			C24r	54.64
CO	Fasic/Zygrh CO	C24r	UNC D			C24r	56.57±01				
LO	T. bramlettei	C24r	UNC D	C24r	55.65	C24r	55.99±15	C24r	54.765		
LRO	T. bramlettei			**C24r**		**C24r**	**56.645**				
HO	F. tympaniformis	C24r	UNC D	C24r	56.02						
LCO	C. eodela	C24r	56.24±03	C24r	56.21						
LCO	Z. bijugatus										
LO	Z. bijugatus									C24r	55.28
HO	E. robusta	C24r	56.62±36					C24r	56.59±03		
LO	D. multiradiatus	C25n	56.98±02	C25n	56.98			C25n	56.76±07	C25n	56.91

TABLE 5, *continued*

LRO = lowest rare occurrence; HO = highest occurrence; HCO = highest common occurrence; AB = acme begin; AE = acme end; XO = cross-over. Bioevents representing the HCO or LCO for a particular taxa are indicated by an asterisk (*). The lowest rare occurrence (LRO), a designation not used in this study but in others, is shown in bold. Unconformities (UNC) are indicated for events located within a hiatus that cannot be accurately dated.

Event	Taxa	Site 1090B		Site 1123C		Bottaccione		Contessa Highway		Site 689B	
		Mag	Date	Mag	Date	Mag	Date	Mag	Date	Mag	Date
AB	Clausicoccus spp.			13r	33.80						
HO	D. saipanensis	C13r	34.25	13r	34.12						
HO	D.barbadiensis	C13r	34.36	13r	34.12						
LO	R. oamaruensis	16n.1n	35.44							15r	35.35
LCO	I. recurvus	C16n.2n	35.98			C16n2n	36.01±.04				
LO	I. recurvus	C16r	36.28					C15r?		C16n	35.99
HO	C. reticulatum	C13r	34.93			C15n?	34.97±.04			16n	35.99
HCO	C. reticulatum	C16n.2n	36.28								
HO	N. dubius			Site 1051A						17n1n	36.54
LO	Ch. oamaruensis	C18n?	38.12	Mag	Date					18n1n	36.98
HO	Ch. grandis	C18n?	38.7			C18n	38.74	C18n	39.14		
HO	S. spiniger			C18n	38.14						
HO	S. radians					C18n	38.74	C18n	39.65		
LO	S. predistentus			C18r	39.84						
LCO	D. bisecta	C18n.1n	39.76	C18r	39.73						
LO	D. bisecta	C18r?	40.05			C18r	39.97	C18n	39.39	17n1n	37.29
HO	Ch. expansus									18n1n	39.33
HO	Ch.solitus	C18r?	39.91	C18r	39.98						
LO	C. reticulatum	C18r?	40.36	C19r	41.27						
LO	R. umblilca			C20n	42.45	C20n	42.56	C20n	42.64		
HO	Ch. gigas			C20r	43.09						
HO	N. fulgens			C20n	42.61	C20n					
LO	Ch. gigas			C20r	45.11						
LO	S. furcatolithoides			C20r	45.11						
LO	D.saipanensis	C18r?	40.05*	C20r	45.17	C21r	47.78	19r	40.91		
LO	N. fulgens			C20r	45.24	C21n	46.49	C21n	46.91		
LO	Nannotetrina spp.			C21n	45.40						
LO	R. inflata			C21n		C21n	47.17				
HO	C.crassus					C22n	48.84	C22n	48.78		
HO	D. lodoensis					C22n	49.15*	C22n	48.78		
HO	D. kuepperii							C22n	48.78		
AE	Discoaster spp.										
AB	Dict/Reticulo gp.										
HO	Toweius spp.										
LO	D. sublodoensis					C22r	50.51	C22n	49.37		
HO	T. orthostylus					C23n	52.34	C22r	50.02		
LO	C. crassus	Site 1262				C23n	51.10	C23n	51.78		
AB	Discoaster spp.										
HO	D. diastypus	Mag	Date	C22r	49.85	C23n	51.10	C22n			
LO	N. dubius			C23r	52.54						
LCO	D. lodoensis			C23n	51.76						
LO	D. lodoensis			C24n	53.35	C24n	53.29	C23r			
LCO	Chiphrag. spp.										
HO	C. eodela			C23r	52.54						
LO	G. gammation			C23r	52.55	C24n		C24n	53.58		
HO	D.multiradiatus	C24r	54.145*	C24r	54.21	C24n	53.06	C24r	53.87		
HO	T. eminens			C24n	53.15						
LO	D. kuepperii							C24r	56.14		
HCO	T. eminens										
HO	T. contortus	C24r	54.04±.01	C24r	54.10	C24r	53.99				
LO	S. radians	C24r	54.09±.01	C24r	53.96	C24r	54.84	C24r	56.66		
LO	S. editus	C24r	54.18±.01								
LO	T. orthostylus	C24r	54.23±.01	C24r	54.10	C24r	53.99	C24r	54.72		
HO	T. brameltteii	C24r	54.27±.01								
LO	D. diastypus	C24r	54.665			C24r	55.26	C24r	56.14		
LO	T. contortus	C24r	54.54±.01	C24r	54.94; 54.61*						
LO	D.barbadiensis					C24r	54.81	C24r	54.72		
HO	Fasiculithus spp.	C24r	55.24±.01					C24r	54.72		
CO	Fasic/Zygrh CO	C24r	55.58	C24r	56.61						
LO	T. bramlettei	C24r	55.075	C24r	56.29						
LRO	T. bramlettei	**C24r**	**55.605**								
HO	F. tympaniformis			C24r	56.50	C24r	54.84	C24r	54.72		
LCO	C. eodela	C24r	55.595								
LCO	Z. bijugatus	C24r	55.59								
LO	Z. bijugatus	C24r	56.405	C24r	56.64			C24r	55.24		
HO	E. robusta	C25n	56.66	C24r	56.64						
LO	D. multiradiatus	C25n	56.76			C24r	56.08	C25n	56.96		

The LO of *Reticulofenestra oamaruensis*: This event is dated significantly younger at Site 762 (34.40 Ma) than reported in the BKSA95 (35.45 Ma) (Table 5). *Reticulofenestra oamaruensis*, which is extremely rare at Site 762, is known to have an affinity to high latitude (Monechi Buccianti and Gardin 2000; Berggren et al 1995) and this delayed appearance may be due to paleogeographic exclusion. Site 762 is located at mid-paleolatitudes (~40-45°S) during the late Eocene, and the distribution of this species may have expanded into these latitudes during Priabonian cooling (text-figure 2).

The LO of *Isthmolithus recurvus*: Two specimens of *I. recurvus* were identified deeper in the section, with these oldest occurrences dated to 36.37±.12 Ma. An *I. recurvus* 'spike' is identified at several localities by Fornaciri et al. (2010) and Agnini et al. (2011) in Chron C17n. These findings are in agreement with data from Hole 762C as well as Site 1090 (Table 5). The LCO of *I. recurvus* within Chron C16n2n at Hole 762C (36.04±.06 Ma), as well as Massignano (Fornaciari et al. 2010), is in much greater agreement with the calibrated age of the BKSA95 timescale (35.98 Ma), suggesting that the date calculated in the BKSA95 is actually representative of the LCO of *I. recurvus*.

The HO of *Cribrocentrum (Reticulofenestra) reticulatum*: We observe a divergence in the HO and HCO of *C. reticulatum* with respect to the BSKA95 (Table 5). The HO of *C. reticulatum* at 189.86 msbf is dated to ~34.20 Ma; however this species becomes rare and sporadic above 199.00 msbf. The depth for the HCO of *C. reticulatum* fits well within the sedimentation curve, derived using isotopic and magnetostratigraphic tie-points, thus this event has been correlated to the BKSA95 at 35.09 Ma.

The LO of *Dictyococcites (Reticulofenestra) bisectus*: The revised age-model derived for Site 762 yields a significantly older date for both the LO (39.96±.13 Ma, Chron C18r) and LCO (39.11± Ma, Chron C18n.2n) of *D. bisectus* than the age provided for the LO in the BKSA95 timescale (37.68 Ma, Chron C17n.3n). Despite this divergence, these dates are in good agreement with data from other localities globally, including ODP Sites 1218, 1172, 1090, 1051, Alano, Bottaccione, Contessa Highway and several localities from Fornaciari et al (2010), all of which report this species from either Chron C18n or Chron C18r (Table 5). This global agreement suggests that *D. bisectus* has good potential as a biostratigraphic marker and should be investigated for consistency in LO and LCO bioevents at these and other sites.

The LO of *Discoaster sublodoensis*: This event is thought to occur too low in the section at Site 762. The corresponding age-depth point falls below the sedimentation curve (text-figure 3), and attempts to bring this event into greater alignment with hiatus C results in a poor fit among other biostratigraphic, isotopic and magnetostratigraphic tie-points. Our age estimates give a significantly older date (50.51±.02 Ma, Chron C22r) than that provided in the BSKA95 (49.41 Ma, Chron C22n). Only specimens with five, straight, pointed rays were identified as *D. sublodoensis,* so it is unlikely that these early forms are misidentified specimens of *D. lodoensis*. A similar distribution to Site 762 is observed at Site 1051, Site 689, Possagno, and Bottaccione, with specimens of *D. sublodoensis* identified in CP10 and CP11, prior to the LCO and base of CP12a. These issues may be resolved with a more focused examination of both taxonomy and stratigraphic distribution, particularly at these sites, to better constrain the utility of this marker taxa.

ADDITIONAL REMARKS

Sedimentation rates derived from the revised age model at Site 762 show considerable differences to those originally calculated (Shipboard Scientific Party 1990). Average rates for the Priabonian are comparable between studies (~1.5cm/ky); however, the original model shows rates of up to ~3cm/ky in the upper Priabonian, considerably higher than our maximum of ~2cm/ky. Weighted averages for rates through the Bartonian are also notably higher in the original analysis than in the current results (~2cm/ky and ~1cm/ky, respectively). The most striking difference between these analyses is seen in the Lutetian. Though the original model shows sedimentation of ~1-2cm/ky throughout most of the Eocene, rates drop considerably through this interval to a weighted average of ~0.5cm/ky. Conversely, our average rate is double this, at ~1cm/ky. Two hiatuses (A and B) have been identified in the Lutetian, totaling ~4.0 myr in duration. This accounts for nearly half of the 8.2 myr long stage, resulting in a doubling of sedimentation rates in the revised age model. Rates for the uppermost Ypresian are also low in the original age model (~0.3cm/ky; 329.5-332.5 mbsf), to accommodate the ~0.9 myr hiatus (332.18 msbf) identified in the revised model. Original sedimentation rates through the remaining Ypresian are comparable to the revised age model, averaging ~2-3cm/ky, until dropping again near the Paleocene-Eocene boundary (<1cm/ky). This decrease in the original sedimentation rate is related to a ~1.8 myr hiatus identified in the revised age model (412.78 msbf), in association with the PETM.

The revised geochronologic model at Site 762 has produced several notable changes in sedimentation rates through the Eocene. Re-analysis of the nannofossil biostratigraphy and magnetostratigraphy has played a key role; however, these changes are primarily due to the incorporation of four stratigraphic hiatuses, totaling ~6.6 myr in duration. These hiatuses cover approximately 25% of the total Eocene time originally thought to be represented at this locality. Though no stratigraphic breaks or significant changes in lithology are seen in Hole 762C, we interpret these hiatuses as stratigraphic unconformities, likely non-depositional and non-erosive, rather than condensed sections during periods of low sedimentation. While it is beyond the scope of this research to discuss and weigh the numerous mechanisms which may be responsible for creating these disconformities, some comparisons can be drawn between our observations and other research.

Third-order sequence boundary dates of Hardenbol et al. (1998) are contained within the age gaps of the hiatuses identified at Site 762 (Table 6): The Lu3 sequence boundary age (42.98 Ma) is contained within disconformity A (42.02-44.22). The Lu1 sequence boundary age (47.47 Ma) is contained within disconformity B (47.01-48.83). Disconformity C (49.79-50.71 Ma) incorporates the sequence boundary ages of both Yp10 (49.78 Ma) and Yp9 (50.13 Ma). Similarly, disconformity D (54.41-56.22 Ma) contains the sequence boundaries of Yp3-Yp1 (55.19, 55.29 and 55.98 Ma, respectively).

Disconformity D is linked to the PETM (Chron C24r), due to the high relative abundance of dissolution resistant taxa such as *D. multiradiatus* and *F. tympaniformis* [Bown and Pearson (2009); Jiang and Wise (2009); Monechi and Angori (2006); Kahn and Aubry (2004)]. Several authors also note a barren interval associated with the CIE, as well as an increase in clay content [Jiang and Wise (2009); Monechi and Angori (2006);

Kahn and Aubry (2004)]. Raffi and Bernardi (2008) provided a synthesis of 18 PETM sites, where the authors attribute these observations to truncation of the basal PETM sequence from acidification and dissolution of carbonate sediments. Similarly, Ali and Hailwood (1995, fig 2) show stratigraphic gaps in mid-Chron C24r across nine sites in SE England, France and Belgium, with these also correlating to disconformity D at Site 762 (text-figure 3).

A paleogeographic and stratigraphic summary of the northwestern Australian margin (Gradstein 1992), suggests that at least part of the stratigraphic record in this region is affected by erosion or non-deposition, and suggests links to the Himalayan orogeny, ocean spreading tectonics, and/or ocean current reorganization. Gradstein (1992) shows a middle Eocene hiatus at the western foot of Exmouth Plateau (Site 766) and on the Argo Abyssal Plain (Site 765). Siesser and Bralower (1992) identify significant gaps in the nannofossil biostratigraphy on the central Exmouth Plateau at Site 763 in the lower and middle Eocene, but suggest continuous sedimentation through this interval at Site 762. Disconformities identified at Site 762 in the present study may be linked to those described by Siesser and Bralower (1992) and Gradstein (1992), and suggests the mechanism was effective over a much larger area, and a wider range of paleodepths across the northwestern Australian margin.

Similarly, an extensive study by Aubry (1995) examined DSDP and ODP Sites in the northern and southern Atlantic Ocean, with these localities showing stratigraphic hiatuses at discrete magnetostratigraphic intervals through the middle Eocene. A striking number of these Sites correlate to disconformities A-C at Site 762: Disconformity A: Chron C20n-C20r - > 20 Sites; Disconformity B: Chron C21n-C21n - > 30 Sites; Disconformity C: Chron C22r - > 20 Sites. Such wide-spread and extensive stratigraphic gaps suggest the deep sea record is not as continuous as once thought, but can contain frequent hiatuses of significant duration. Many stratigraphic sections likely contain such hiatuses, but have not been identified due to the lack of multidisciplinary integration. Such relationships can be critical to paleoceanographic research, and re-examination of older sedimentation models will likely show additional regions with widespread deep-water hiatuses. Accurate mechanisms, such as eustacy, tectonics, and ocean current reorganization, can only be determined once such sections are accurately interpreted.

CONCLUSIONS

Integration of calcareous nannofossil biostratigraphy and stable isotope geochemistry led to a re-examination of the existing magnetostratigraphy for Hole 762C. This reexamination confirmed four stratigraphic discontinuities and produced and updated age-model for the Hole 762C succession. The magnetostratigraphy of Galbrun (1992) was re-interpreted using this revised nannofossil biostratigraphy, as well as planktonic foraminiferal data and stable isotopic data, resulting in considerable adjustment to magnetic reversal boundaries (text-figure 2). These magnetostratigraphic calibration points, as well as isotopic data and nannofossil bioevents, were combined to produce an integrated age-depth plot calibrated to the GPTS of Ogg Ogg and Gradstein (2008). We identify four hiatuses of ~1-2 myr each in duration. Incorporation of these hiatuses into the depositional model results in a significant increase in sedimentation rates through the Lutetian and portions of the Ypresian. Dates for several nannofossil bioevents are also derived using these new sedimentation rates, and are compared to events from the BKSA95, as well as several, globally distributed sites. Most nannofossil bioevents at Hole 762C are in good agreement with the BKSA95; however, a select number of events at Hole 762C show some offset from that biochronology (LO *R. oamaruensis*, LO/LCO *I. recurvus*, HO/HCO *C. reticulatum*, LO *D. sublodoensis*) or from additional sites (HO *S. radians*), where no date is provided by BKSA95. The most notable and consistent divergence is seen in the LO of *Dictyococcites bisectus*, observed at Site 762 approximately 2 myr before that of the BKSA95. This early occurrence is also observed at Alano, Bottaccione, Contessa Highway, and ODP Sites 1218, 1172, 1090 and 1051, suggesting that the age provided in the BKSA95 is actually representativeof the LCO of *D. bisectus*. Similar discrepancies are observed for the LO of *Discoaster sublodoensis*, observed at Site 762 ~1 myr before the BKSA95, and indicates a need for detailed recalibration of these nannofossil datums.

TABLE 6
Hiatus Summary: summary of unconformities identified at Site 762C, including the event depth, upper and lower extrapolated ages, and approximate duration of the stratigraphic hiatus.

UNC.	Depth (msbf)	Upper Date (Ma)	Lower Date (Ma)	Duration (My)	Associated Sequence
A	289.75	42.02	44.22	2.20	Lu3
B	321.13	47.10	48.83	1.74	Lu1
C	332.18	49.79	50.71	0.92	Yp9-Yp10
D	412.78	54.41	56.22	1.81	Yp1-Yp3

ACKNOWLEDGMENTS

This research used samples and data provided by the Ocean Drilling Program (ODP). The ODP is sponsored by the National Science Foundation (NSF) and participating countries under the management of Joint Oceanographic Institutions (JOI) Inc. The authors would like to thank Mary Anne Holmes, Tracy Frank (University of Nebraska-Lincoln, Geosciences) and Paul Hanson (UN-L, School of Natural Resources), Agata Di Stephano (Universita' Degli Studi di Catania) as well as one anonymous reviewer for their collaboration and revisions, which greatly improved this manuscript

REFERENCES

ACHUTHAN, M. V. and STRADNER, H., 1969. Calcareous nannoplankton from the Wemmelian stratotype. *In:* Bronnimann, P. and Renz, H. H., Eds. *Proceedings First International Conference on Planktonic Microfossils, Geneva, Volume 1,*1–13. Leiden: EJ Brill.

AGNINI, C., FORNACIARI, E., RAFFI, I., RIO, D., RÖHL, U. and WESTERHOLD, T., 2007. High resolution nannofossil biochronology of middle Paleocene to early Eocene at ODP Site 1262: Implications for calcareous nannoplankton evolution. *Marine Micropaleontology*, 64: 215–248.

AGNINI, C., MUTTONI, G., KENT, D. V. and RIO, D., 2006. Eocene biostratigraphy and magnetic stratigraphy from Possango, Italy: the calcareous nannofossil response to climate variability. *Earth and Planetary Science Letters*, 241: 815–830.

ALI, J. R. and HAILWOOD, E. A., 1995. Magnetostratigraphy of upper Paleocene through lower middle Eocene strata of Northwest Europe. In: Berggren, W. A., Kent, D., V., Aubry, M.–P. and Hardenbol, J.,

Eds., *Geochronology, time scales and global stratigraphic correlations.* Society for Sedimentary Geology (SEPM) Special Publication, 54: 275–280.

AUBRY, M.–P., 1995. From chronology to stratigraphy: interpreting the lower and middle Eocene stratigraphic records in the Atlantic Ocean. In: Berggren, W. A., Kent, D., V., Aubry, M.–P. and Hardenbol, J., Eds., *Geochronology, time scales and global stratigraphic correlations,* 213–274. Tulsa, OK: Society for Sedimentary Geology (SEPM). Special Publication 54:.

AUBRY, M.–P., 1991. Sequence stratigraphy: Eustacy or tectonic imprint? *Journal of Geophysical Research*, 96: 6641–6679.

BERGGREN, W. A. and PEARSON, P. N., 2005. A revised tropical to subtropical Paleogene planktonic foraminiferal zonation. *Journal of Foraminiferal Research*, 35: 279–298.

BERGGREN, W. A., KENT, D. V., AUBRY, M.–P. and HARDENBOL, J., Eds., 1995a. *Geochronology, time scales and global stratigraphic correlations.* Tulsa, OK: Society for Sedimentary Geology (SEPM) Special Publication 54.

BERGGREN, W. A., KENT, D. V., SWISHER, C. C. III and AUBRY, M.–P., 1995b. A revised Cenozoic geochronology and chronostratigraphy. In: Berggren, W. A. et al., Eds., *Geochronology, time scales and globalstratigraphic correlation,* 129–212. Tulsa, OK: Society of Sedimentary Geology (SEPM). Special Publication 54.

BERGGREN, W. A. and MILLER, K. G., 1988. Paleogene tropical planktonic foraminiferal biostratigraphy and magnetostratigraphy. *Micropaleontology,* 34: 362–380.

BLEIL, U., 1985. The magnetostratigraphy of northwest Pacific sediments, Deep Sea Drilling Project Leg 86. *In*: Heath, G. R., Burckle, L. H. et al. (Eds.), *Initial Reports of the Deep Sea Drilling Project, Leg 86.* 441–458. Washington DC: U. S. Govt. Printing Office. doi:10.2973/dsdp. proc.86.117.1985

BOHATY, S. M. and ZACHOS, J. C., 2003. Significant Southern Ocean warming event in the late middle Eocene. *Geology*, 31: 1017–1020.

BOHATY, S. M., ZACHOS, J. C., FLORINDO, F. and DELANEY, M. L., 2009. Coupled greenhouse warming and deep–sea acidification in the Middle Eocene. *Paleoceanography*, 24: PA2207. 10.1029/2008PA001676

BOLLI, H. M., 1957. The genera *Globogerina* and *Globorotalia* in the Paleocene–Lower Eocene Lizard Springs Formation of Trinidad, B. W. I. *Bulletin of the U. S. National Museum,* 215: 61–82.

BOWLES, J., 2006. Data report: revised magnetostratigraphy and magnetic mineralogy of sediments from Walvis Ridge, Leg 208. In: Kroon, D., Zachos, J. C. and Richter, C. *Proceedings of the Ocean Drilling Program: Scientific Results, 208,* 24pp. College Station, TX: Ocean Drilling Program. doi:10.2973/odp.proc.sr.208.206.2006

BOWN, P. R. and PEARSON, P., 2009. Calcarous plankton evolution and the Paleocene/Eocene Thermal Maximum event: new evidence from Tanzania. *Marine Micropaleontology*, 71: 60–70.

BOWN, P. R. and YOUNG, J. R., 1998. Techniques. In: Bown, P. E., Ed., *Calcareous nannofossil biostratigraphy,* 16–28. London: Kluwer Academic.

BRAMLETTE, M. N. and RIEDEL, W. R., 1954. Stratigraphic value of discoasters and some other microfossils related to recent coccolithophores. *Journal of Paleontology*, 28: 385–403.

BRAMLETTE, M. N. and SULLIVAN, F. R., 1961. Coccolithophorids and related nannoplankton fossils between the Maestrichtian and Danian. *Micropaleontology*, 7: 129–174.

BRAMLETTE, M. N. and WILCOXON, J. A., 1967. Middle Tertiary calcareous nannoplankton of the Cipero Section, Trinidad. *Tulane Studies in Geology*, 5: 93–131.

BRÖNNIMANN, P. and STRADNER, H., 1960. Die Foraminiferen– und Discoasteridenzonen von Kuba und ihre interkontinentale Korrelation. *Erdoel–Zeitschrift*, 76: 364–369.

BUKRY, D., 1971a. Cenozoic calcareous nannofossils from the Pacific Ocean. *Transactions of the San Diego Society of Natural History,* 16: 303–327.

———, 1971b. Discoaster evolutionary trends. *Micropaleontology*, 17: 43–52.

———, 1972. Further comments on coccolith stratigraphy, Leg 12, Deep Sea Drilling Project. *In*: Laughton, A. S., Berggren, W. A., et al., *Initial Reports of the Deep Sea Drilling Project, Leg 12,* 1071–1083. Washington, DC: U. S. Government Printing Office.

BUKRY, D. and PERCIVAL, S. F., 1971. New Tertiary calcareous nannofossils. *Tulane Studies in Geology and Paleontology*, 8: 123–146.

BYBELL, L. M. and SELF–TRAIL, J. M., 1994. *Evolutionary, biostratigraphic, and taxonomic study of calcareous nannofossils from a continuous Paleocene–Eocene boundary section in New Jersey*. Washington, DC: U. S. Geological Survey Professional Paper 1554, 36 pp.

CAMPBELL, R. J., HOWE, R. W. and REXILIUS, J. P., 2004. Middle Campanian–lowermost Maastrichtian nannofossil and foraminiferal biostratigraphy of the northwestern Australian margin. *Cretaceous Research*, 25: 827–864.

CANDE, S. C. and KENT, D. V., 1995. Revised calibration of the geomagnetic polarity time scale for the Late Cretaceous and Cenozoic. *Journal of Geophysical Research*, 100(B4): 6093–6096. doi:10.1029/94JB03098

CATANZARITI, R., RIO, D. AND MARTELLI, L., 1997. Late Eocene to Oligocene calcareous nannofossil biostratigraphy in the northern Appennines: the Ranzano sandstone. *Memorie di Scienze Geologiche*, 49:207-253.

CHANNEL, J. E. T., GALEOTTI, S., MARTIN, E. E., BILLUPS, K., SCHER, H. D. and STONER, J. S., 2003. Eocene to Miocene magnetostratigraphy, biostratigraphy, and chemostratigraphy at ODP Site 1090. *Geological Society of America Bulletin*, 115: 607–623.

CRAMER, B. S., TOGGWEILER, J. R., WRIGHT, J, D., KATZ, M. E. and MILLER, K. G., 2009. Ocean overturning since the Late Cretaceous: Inferences from a new benthic foraminiferal isotope compilation. *Paleoceanography*, 24: 14pp. PA4216 doi:10.1029/2008PA001683,

CRAMER, B. S., WRIGHT, J. D., KENT, D. V. and AUBRY, M.–P., 2003. Orbital climate forcing of δ13C excursions in the late Paleocene–early Eocene (Chrons C24n –C25n). *Paleoceanography*, 18: 25 pp. 1097. doi:10.1029/2003PA000909

DEFLANDRE G. and FERT, C., 1954. Observations sur les Coccolithophoridés actuels et fossiles en microscopie ordinaire et électronique. *Annales de. Paléontologie*, 40: 115–176.

APPENDIX 1

Nannofossil Sample List: Sample intervals and depths (mbsf) for calcareous nannofossil biostratigraphy. Samples used in detailed assemblage study marked with asterisks (*), with remaining samples used for greater control of biostratigraphic markers.

Appendix A: Nannofossil Sample List, ODP Hole 762C

1*	3/4/1949	184.49	48	10-4-120	2517	95	16-2-52	303.52	142	22-2-125	362.75
2*	3-4-101	185.01	49*	11/1/1950	256	96*	16-2-125	304.25	143*	22-3-52	363.52
3*	4-1-46.5	189.47	50	11-1-125	256.75	97*	16-3-52	306.52	144	22-3-125	364.25
4*	4-1-123.5	190.24	51*	11/2/1950	257.5	98	16-3-125	307.25	145*	22-4-47.5	364.98
5*	4/2/1950	191	52	11-2-125	258.25	99*	16-4-45	307.95	146	22-4-125	365.75
6*	4-2-126.5	19177	53	11-3-51.5	259.02	100*	17-1-51	313.01	147*	22-5-46	366.46
7*	4/3/1950	192.5	54*	11-3-125	259.75	101	17-1-145	313.95	148	22-5-125	367.25
8*	4-3-100	193	55*	11/4/1950	260.5	102*	17-2-52	314.52	149*	22-6-53	368.03
9*	4/4/1950	194	56	11-4-125	26125	103	17-2-125	315.25	150	22-6-110	368.6
10	4-4-147	194.97	57*	11/5/1950	262	104	17-3-52	316.02	151*	23-1-49.5	370
11*	5/1/1950	199	58	11-5-125	262.75	105*	17-3-125	316.75	152*	23-1-125	370.75
12	5-1-125	199.75	59*	11/6/1950	263.5	106*	17-4-52	317.52	153*	23-2-49	37149
13	5/2/1953	200.53	60	11-6-140	264.4	107	17-4-116..5	318.17	154	23-2-113	372.13
14*	6/1/1948	208.48	61*	12/1/1951	265.51	108*	17-5-49.5	319	155*	23-3-51	373.01
15	6-1-125	209.25	62	12-1-125	266.25	109	17-5-148	319.98	156*	24-1-54	379.54
16*	6/2/1946	209.96	63*	12/2/1951	267.01	110*	18-1-50	322.5	157	24-1-142	378.42
17	6-2-125	210.75	64	12-2-125	267.75	111	18-1-124.5	323.25	158*	25-1-50.5	389.01
18*	6/3/1950	211.5	65*	12/3/1950	268.5	112*	18-2-50	324	159	25-1-125	389.75
19	6-3-125	212.25	66	12-3-125	269.25	113	18-2-125	324.75	160*	25-2-47.5	390.48
20*	6/4/1950	213	67*	12/4/1950	270	114	18-3-50.5	325.51	161	25-2-115	391.15
21	6-4-125	213.75	68	12-4-125	270.75	115*	18-3-125	326.25	162*	25-3-52	392.02
22*	6/5/1940	214.4	69*	12/5/1950	2715	116*	18-4-53	327.03	163	25-3-125	392.75
23*	7/1/1950	218	70	12-5-125	272.25	117	18-4-125	327.75	164	25-4-54	393.54
24	7-1-125	218.75	71	12/6/1950	273	118*	18-5-50	328.5	165*	25-4-125	394.25
25	7/2/1954	219.54	72*	12-6-147	273.97	119	18-5-125	329.25	166	25-5-43	394.93
26*	7-2-125	220.25	73*	13-1-50	275	120*	18-6-52	330.02	167*	26-1-49	398.3
27	7/3/1950	221	74	13-1-125	275.75	121	18-6-148.5	330.99	168	26-1-125	398.77
28*	7-3-119	22169	75*	13-2-71	276.71	122	19-1-52	33152	169*	26-2-49	399.17
29	7/4/1950	222.5	76*	14-1-5	284.05	123*	19-1-125	332.75	170	26-2-125	399.69
30*	7-4-146	223.46	77	14-1-72.5	284.73	124*	19-2-52	333.52	171*	26-3-51	400.16
31	8/1/1950	227.5	78*	14-2-50	286	125	19-2-125	334.25	172	26-3-125	400.62
32*	8-1-125	228.25	79	14-2-125	286.75	126*	19-3-53	335.03	173*	26-4-47	40106
33*	8/2/1953	229.03	80	14-3-52.5	287.53	127	19-3-125	335.75	174	26-4-113.5	40147
34	8-2-126	229.76	81*	14-3-126	288.26	128*	19-4-52	336.52	175*	26-5-50	402.01
35	8/3/1952	230.52	82*	14-4-55	289.05	129*	20-1-50	3415	176	26-5-148.5	402.61
36*	8-3-125	23125	83	14-4-125	289.75	130	20-1-125	342.25	177*	27-1-50	403
37*	8/4/1950	232	84*	14-5-50	290.5	131*	20-2-50	343	178	27-1-125	403.75
38	8-4-125	232.75	85	14-5-115	29115	132	20-2-115	343.65	179*	27-2-50	404.5
39*	8/5/1950	233.5	86*	14-6-50	292	133*	20-3-52	344.52	180	27-2-125	405.25
40*	9/1/1946	236.96	87	14-6-147	292.97	134	20-3-125	345.25	181*	27-3-50	406
41*	10/1/1950	246.5	88*	15-1-48	293.98	135*	20-4-47.5	345.98	182	27-3-125	406.75
42	10-1-125	247.25	89	15-1-125	294.75	136*	21-1-50	351	183*	27-4-50	407.5
43*	10-2-49.5	248	90	15-2-52	295.52	137	21-1-129	35179	184	27-4-138	408.38
44	10-2-125	248.75	91*	15-2-124	296.24	138*	21-2-50	352.2	185*	28-1-59	412.59
45*	10/3/1950	249.5	92*	15-3-48	296.98	139*	22-1-50	360.5	186*	28-1-125	413.25
46	10-3-115	250.15	93*	16-1-48	303.48	140	22-1-125	36125	187*	29-1-50	422
47*	10/4/1950	251	94	16-1-125	304.25	141*	22-2-46	36196			

APPENDIX 2
Taxonomic List - Calcareous Nannofossils.

Appendix B: Taxonomic List - Calcareous Nannofossil

*References for calcareous nannofossil taxonomy can be found in Perch-Nielsen 1985

Genus/Species	Original Reference	Secondary Reference
Campylosphaera eodela	Bukry & Percival 1971	
Clausicoccus spp.	Prins 1979	
Clausicoccus subdistichus	Roth & Hay, *in* Hay et al. 1967	Prins 1979
Chiasmolithus expansus	Bramlette & Sullivan 1961	Gartner 1970
Chiasmolithus gigas	Bramlette & Sullivan 1961	Radomski 1968
Chiasmolithus grandis	Bramlette & Riedel 1954	Radomski 1968
Chiasmolithus oamaruensis	Deflandre *in* Deflandre & Fert 1954	Hay, et al. 1966
Chiasmolithus solitus	Bramlette & Sullivan 1961	Locker 1968
Chiphragmolithus spp.	Bramlette & Sullivan 1961	
Coccolithus crassus	Bramlette & Sullivan 1961	
Cribrocentrum erbe	Fornaciari et al. 2010	
Cribrocentrum isabellae	Fornaciari et al. 2010	
Cribrocentrum reticulatum	Gartner & Smith 1967	Perch-Nielsen 1971a
Dictyococcites bisectus	Hay Mohler & Wade 1966	Bukry & Percival 1971
Discoaster spp.	Tan 1927	
Discoaster barbadiensis	Tan 1927	emend. Bramlette & Riedel 1954
Discoaster bifax	Bukry 1971a	
Discoaster diastypus	Bramlette & Sullivan 1961	
Discoaster kuepperi	Stradner 1959	
Discoaster lodoensis	Bramlette & Riedel 1954	
Discoaster multiradiatus	Bramlette & Riedel 1954	
Discoaster nobilis	Martini 1961	
Discoaster saipanensis	Bramlette & Riedel 1954	
Discoaster sublodoensis	Bramlette & Sullivan 1961	
Ericsonia robusta	Bramlette & Sullivan 1961	Perch-Nielsen 1977
Fasciculithus spp.	Bramlette & Sullivan 1961	
Fasciculithus tympaniformis	Hay & Mohler, *in* Hay et al. 1967	
Girgisia gammation	Bramlette & Sullivan 1961	Varol 1989
Isthmolithus recurvus	Deflandre *in* Deflandre & Fert 1954	
Nannotetrina spp.	Achuthan & Stradner 1969	
Nannotetrina alata	Martini 1960 *in* Martini & Stradner 1960	Haq & Lohmann 1976
Nannotetrina fulgens	Stradner *in* Martini & Stradner 1960	Achuthan & Stradner 1969
Neococcolithus dubius	Deflandre *in* Deflandre & Fert 1954	
Reticulofenestra oamaruensis	Deflandre *in* Deflandre & Fert 1954	Stradner *in* Haq 1968
Reticulofenestra umbilica	Levin 1965	Martini & Ritzkowski 1968
Rhabdosphaera gladius	Locker 1967	
Rhabdosphaera inflata	Bramlette & Sullivan 1961	
Rhomboaster spp.	Bramlette & Sullivan 1961	
Sphenolithus editus	Perch-Nielsen *in* Perch-Nielsen et al. 1978	
Sphenolithus furcatolithoides	Locker 1967	emend. Shamrock 2010
Sphenolithus predistentus	Bramlette & Wilcoxon 1967	
Sphenolithus radians	Deflandre *in* Grassé 1952	
Sphenolithus spiniger	Bukry 1971a	
Toweius spp.	Hay & Mohler 1967	
Toweius eminens	Bramlette & Sullivan 1961	Perch-Nielsen 1971b
Tribrachiatus? *bramlettei*	Brönnimann & Stradner 1960	Bybell & Self-Trail 1995
Tribrachiatus contortus	Stradner 1958	Bukry 1972
Tribrachiatus orthostylus	Bramlette & Riedel 1954	Shamrai 1963
Zygrhablithus bijugatus	Deflandre *in* Deflandre & Fert 1954	

FLORINDO, F. and ROBERTS, A. P.2005. Eocene–Oligocene magnetobiochronology of ODP Sites 689 and 690, Maud Rise, Weddell Sea, Antarctica. *Geological Society of America Bulletin*, 117: 46–66.

GALBRUN, B., 1992. Magnetostratigraphy of Upper Cretaceous and lower Tertiary sediments, Sites 761 and 762, Exmouth Plateau, northwest Australia. In: Rad, U. von, Haq, B. U. et al., *Proceedings of the Ocean Drilling Project, Scientific Results, 122,* 699–716. College Station, TX: Ocan Drilling Program.

GAELOTTI, S., KRISHNAN, S., PAGANI, M., LANCI, L., GAUDIO, A., ZACHOS, J. C., MONECHI, S., MORELLI, G. and LOURENS, L., 2010. Orbital chronology of Early Eocene hyperthermals from the Contessa Road section, central Italy. *Earth and Planetary Science Letters*, 290: 192–200.

GARTNER, S. Jr., 1970. Phylogenetic lineages in the Lower Tertiary coccolithus genus *Chiasmolithus*. In: Yochelson, E. L., Ed., *North American Paleontological Convention, Sept. 1969. Proceedings G*: 930–957. Lawrence, KS: Allen Press.

GARTNER S., Jr. and SMITH L. A., 1967. Coccoliths and related calcareous nannofossils from the Yazoo Formation (Jackson, late Eocene) of Louisiana. *University of Kansas Paleontological Contributions*, 20: 1–7

GOLOVCHENKO, X., BORELLA, P. E. and O'CONNELL, S, 1992. Sedimentary cycles on the Exmouth Plateau. In: Rad, U. von, Haq, B. U. et al., *Proceedings of the Ocean Drilling Program: Scientific Results, 122*: 279–291. College Station, TX: Ocean Drilling Program. doi:10.2973/odp.proc.sr.122.141.1992.

GRADSTEIN, F. M., 1992. Legs 122 and 123, northwestern Australian margin—a stratigraphic and paleogeographic summary. In: Gradstein, F. M., Ludden, J. N. et al., *Proceedings of the Ocean Drilling Program: Scientific Results, 123,* 801–816. College Station, TX: Ocean Drilling Program. doi:10.2973/odp.proc.sr.123.110.1992

GRADSTEIN, F., OGG, J. and SMITH, A., 2004. *A geologic time scale 2004*. Cambridge: Cambridge University Press, 589pp.

GRASSÉ, P. P., 1952. *Traité de Zoologie, Anatomie, Systématique, Biologie. Vol.1, fasc.1: Phylogénie. Protozoaires: généralités. Flagellés.* Paris: Masson et cie.

HAQ, B. U., 1968. Studies on Upper Eocene calcareous nannoplankton from NW Germany. *Stockholm Contributions in Geology*, 18: 13–74.

HAQ, B. U. and LOHMANN, G. P., 1976. Early Cenozoic calcareous nannoplankton biogeography of the Atlantic Ocean. *Marine Micropaleontology*, 1: 119–194.

HAQ, B. U., BOYD, R. L., EXON, N. F. and RAD, U. VON, 1992. Evolution of the central Exmouth Plateau: a post–drilling perspective. In: Rad, U. von, Haq, B. U. et al., *Proceedings of the Ocean Drilling Program: Scientific Results, 122,* 801–818. College Station, TX: Ocean Drilling Program. doi:10.2973/odp.proc.sr.122.182.1992

HAQ, B. U., RAD, U. VON, O'CONNELL, S. et al*.,* 1990. *Proceedings of the Ocean Drilling Program: Initial Reports, 122,* 826pp. College Station, TX: Ocean Drilling Program. doi:10.2973/odp.proc.ir.122.1990

HARDENBOL, J., THIERRY, J., FARLEY, M. B., JACQUIN, T. and GRICIANSKY, P.–C. DE, 1998. *Mesozoic and Cenozoic sequence stratigraphy of European basins.* Tulsa, OK: Society for Sedimentary Geology (SEPM). Special Publication 60, 786 pp.

HAY, W. W. and MOHLER, H. P., 1967. Calcareous Nannoplankton from Early Tertiary Rocks at Pont Labau, France, and Paleocene–Early Eocene correlations. *Journal of Paleontology*, 41(6): 1505–1541, pls.196–206.

HAY, W. W., MOHLER, H. P. and WADE, M. E., 1966. Calcareous nannofossils from Nal'chik (Northwest Caucasus). *Eclogae Geologicae Helvetiae*, 59: 379–399.

HAY, W. W., MOHLER, H. P., ROTH, P. H., SCHMIDT, R. R. and BOUDREAUX, J. E., 1967. Calcareous nannoplankton zonation of the Cenozoic of the Gulf Coast and Caribbean–Antillean area, and transoceanic correlation. *Transactions of the Gulf Coast Association of Geologic Societies*, 17: 428–480.

JIANG, S. and WISE, S. W., JR, 2009. Distinguishing the influence of diagenesis on the paleoecological reconstruction of nannoplankton across the Paleocene/Eocene Thermal Maximum: An example from the Kerguelen Plateau, southern Indian Ocean. *Marine Micropaleontology*, 72: 49–59.

JOVANE, L., FLORINDO, F., COCCIONI, R., DINARES–TURELL, J., MARSILI, A., MONECHI, S., ROBERTS, A. P. and SPROVIERI, M., 2007. The middle Eocene climatic optimum event in the Contessa Highway section, Umbrian Apennines, Italy. *Geological Society of America Journal*, 119: 413–427. doi:10.1130/1325917.1

KAHN, A. and AUBRY, M.–P., 2004. Provincialism associated with the Paleocene/Eocene thermal maximum: temporal constraint. *Marine Micropaleontology*, 52: 117–131.

LEVIN H. L., 1965, Coccolithophoridae and related microfossils from the Yazoo Formation (Eocene) of Mississippi. *Journal of Paleontology*, 39: 265–272.

LOCKER, S., 1967. Neue Coccolithophoriden aus dem Alttertiär Norddeutschlands. *Geologie*, 16: 361–364.

————, 1968. Biostratigraphie des Alttertiärs von Norddeutschland mit Coccolithophoriden: *Monatsberichte der Deutschrn Akademie der Wissenschat zu Berlin*, 10: 220–229.

LOURENS, L. J., SLUIJS, A., KROON, D., ZACHOS, J. C., THOMAS, E., ROHL, U., BOWLES, J. and RAFFI, I., 2005. Astronomical pacing of late Paleocene to early Eocene global warming events. *Nature*, 435: 1083–1087.

LOWRIE, W., ALVAREZ, W., NAPOLEONE, G., PERCH–NIELSEN, K., PREMOLI SILVA, I. and TOUMARKINE, M., 1982. Paleogene magnetic stratigraphy in Umbrian pelagic carbonate rocks: the Contessa sections, Gubbio. *Geological Society of America Bulletin*, 93: 414–432.

LYLE, M. W., WILSON, P. A., JANECEK, T. R. et al., 2002. Leg 199 summary. *Proceedings of the Ocean Drilling Program:Initial Reports, 199*, 1–87. College Station, TX: Ocean Drilling Program.

MARINO, M. and FLORES, J.–A., 2002a. Data report: calcareous nannofossil data from the Eocene to Oligocene, Leg 177, Hole 1090B. In: Gersonde, R., Hodell, D. A. and Blum, P., *Proceedings of the Ocean Drilling Program Scientific Results*, *177*, 14pp. College

APPENDIX C

Taxonomic List – Planktonic Foraminifera.

Genus/Species	Reference
Morozovella aragonensis	Nuttall 1930
Morozovella formosa	Bolli 1957
Turborotalia pomeroli	Toumarkine & Bolli 1970

Station, TX: Ocean Drilling Program. doi:10.2973/odp.proc.sr.177.115.2002

———, 2002b. Middle Eocene to early Oligocene calcareous nannofossil stratigraphy at Leg 177 Site 1090. *Marine Micropaleontology,* 25: 383–398.

MARTINI, E., 1961. Nannoplankton aus dem Tertiär und der obersten Kreide von SW–Frankreich. *Senckenbergiana Lethaea*, 42: 1–32.

———, 1971. Standard Tertiary and Quaternary calcareous Nannoplankton zonation. In: Farinacci, A., Ed., *Proceedings of the Second Planktonic Conference, Roma, 1970*, *2,* 739–785. Rome: Edizioni Tecnoscienza.

MARTINI, E. and RITZKOWSKI, S., 1968. Die Grenze Eozän/Oligozän in der Typus–Region des Unteroligozäns (Helmstedt–Egeln–Latdorf). *Mem. Bur. Rech. Geol. Minieres*, 69: 233–237.

MARTINI, E. and STRADNER, H., 1960. Nannotetraster eine stratigraphisch bedeutsame neue Discoasteridengattung. *Erdoel–Zeitschrift*, 8: 266–270.

MCGONIGAL, K. and STEFANO, A. DI, 2002. Calcareous nannofossil biostratigraphy of the Eocene–Oligocene transition, ODP Sites 1123 and 1124. In: Richter, C., *Proceedings of the Ocean Drilling Program Scientific Results*, *181*: 207–239. doi:10.2973/odp.proc.sr.181.207.2002

MILLER, K. G., KENT, D. V., BROWER, A. N., BYBELL, L. M., FEIGENSON, M. D., OLSSON, R. K. and POORE, R. Z., 1990. Eocene–Oligocene changes on the New Jersey coastal plain linked to the deep–sea record. *Geological Society of America Bulletin*, 102: 331–339.

MITA, I., 2001. Data report: Early to Late Eocene calcareous nannofossil assemblages of Site 1051 and 1052, Blake Nose, northwestern Atlantic Ocean. *In*: Kroon, D., Norris, R. D. and Klaus, A., *Proceedings of the Ocean Drilling Program: Scientific Results, 171B,* 122–150. College Station, TX: Ocean Drilling Program.

MONECHI, S, 1985. Campanian to Pleistocene calcareous nannofossil stratigraphy from the northwest Pacific Ocean, Deep Sea Drilling Project Leg 86. *In*: Heath, G. R., Burckle, L. H. et al., *Initial Reports of the Deep Sea Drilling Program, Leg 86,* 301–336. Washington, DC: U. S. Government Printing Office. doi:10.2973/dsdp.proc.86.110.1985

MONECHI, S. and ANGORI, E., 2006. Data report: calcareous nannofossil biostratigraphy of the Paleocene/Eocene boundary, Ocean Drilling Program Leg 208 Hole 1266C. In: Kroon, D., Zachos, J. C. and Richter, C., *Proceedings of the Ocean Drilling Program: Scientific Results, 208,* 9pp. College Station, TX: Ocean Drilling Program. doi:10.2973/odp.proc.sr.208.2006

MONECHI, S. and THIERSTEIN, H. R., 1985. Late Cretaceous–Eocene nannofossil and magnetostratigraphic correlations near Gubbio, Italy. *Marine Micropaleontology*, 9: 419–440.

MONECHI, S., BUCCIANTI, A. and GARDIN, S., 2000. Biotic signals from nannoflora across the iridium anomaly in the upper Eocene of the Massignano section: evidence from statistical analysis. *Marine Micropaleontology*, 39: 219–237.

NAPOLEONE, G., PREMOLI SILVA, I., HELLER, F., CHELI, P., COREZZI, S. and FISCHER, S. G., 1983. Eocene magnetic stratigraphy at Gubbio, Italy, and its implications for Paleogene geochronology. *Geological Society of America Bulletin*, 94: 181–191.

NEAL, J. E. and HARDENBOL, J., 1998. Introduction to the Paleogene. *In*: de Graciansky, P.–C., Hardenbol, J., Jaquin, T. and Vail, P. R., *Mesozoic and Cenozoic sequence stratigraphy of European Basins,* 87–90. Tulsa, OK: Society for Sedimentary Geology (SEPM). Special Publication 60:.

NICOLO, M. J., DICKENS, G. R., HOLLIS, C. J. and ZACHOS, J. C., 2007. Multiple early Eocene hyperthermals: Their sedimentary expression on the New Zealand continental margin and in the deep sea. *Geology,* 35: 699–702.

NUTTALL, W. L. F., 1930. Eocene foraminifera from Mexico. *Journal of Paleontology*, 4: 271–293.

OGG, J. G. and BARDOT, L., 2001. Aptian through Eocene magnetostratigraphic correlation of the Blake Nose Transect (Leg 171B), Florida continental margin. In: Kroon, D., Norris, R. D. and Klaus, A., Proceedings of the Ocean *Drilling Program: Scientific Results, 171B*, 58pp. doi:10.2973/odp.proc.sr.171b.104.2001

OGG, J. G, OGG, G. and GRADSTEIN, F. M., 2008. *The concise geologic time scale.* Cambridge: Cambridge University Press, 177 pp.

OKADA, H. and BUKRY, D., 1980. Supplementary modification and introduction of code numbers to the lowlatitude coccolith biostratigraphic zonation (Bukry, 1973, 1975). *Marine Micropaleontology*, 5: 321–325.

PÄLIKE, H., NORRIS, R. D., HERRLE, J. O., WILSON, P. A., COXALL, H. K., LEAR, C. H., SHACKLETON, N. J., TRIPATI, A. K. and WADE, B. S., 2006. The heartbeat of the Oligocene climate system. *Science,* 314: 1894–1898. doi:10.1126/science.1133822

PEARSON, P. N., MCMILLAN, I. K., WADE, B. S., DUNKLEY JONES, T., COXALL, H. K., BOWN, P. R. and LEAR, C. H., 2008. Extinction and environmental change across the Eocene–Oligocene boundary in Tanzania. *Geology*, 36: 179–182.

PERCH–NIELSEN, 1971a. Elektronenmikroskopiche Untersuchungen an coccolithen und ver wandten Formen aus dem Eozân von Dänemark. *Det Kongelige Danske Videnskabernes Selskab biologie Skrifter,*18: 1–76.

———, 1971b. Einige neue Coccolithen aus dem Paläozän der Bucht von Biskaya. *Bulletin of the Geological Society of Denmark*, 21: 347–361.

———, 1977. Albian to Pleistocene calcareous nannofossils from the Western South Atlantic, DSDP Leg 39. In: Supko, P. R., Perch–Nielsen, K. et al., 1977. *Initial Reports of the Deep Sea Drilling Project, Leg 39*, 699–823. Washington, DC: U. S. Government Printing Office.

———, 1985. Cenozoic calcareous nannofossils. In: Bolli, H. M., Saunders, J. B. and Perch–Nielsen, K., Eds., *Plankton stratigraphy*, 427–554. Cambridge: Cambridge University Press.

PERCH–NIELSEN K., SADEK A., BARAKAT M. G. and TELEB F., 1978. Late Cretaceous and Early Tertiary calcareous nannofossil and planktonic foraminifera zones from Egypt. In: Actes du VI Colloque Africain de Micropaléontologie. Tunis: *Annales des Mines et de la Géologie*, 28(2): 337–403.

PRINS, B., 1979. Notes on nannology – 1. *Clausicoccus*, a new genus of fossil coccolithophorid. *International nannoplankton Association (INA) Newsletter*, 1: N2 – N4.

RAD, U. VON, HAQ, B. U. et al., 1992. *Proceedings of the Ocean Drilling Program: Scientific Results, 122,* 934pp. College Station, TX: Ocean Drilling Program. doi:10.2973/odp.proc.sr.122.1992

RADOMSKI, A., 1968. Calcareous nannoplankton zones in Paleogene of the western Polish Carpatians. *Rocznik Polskiego Towarzystwa Geologicznego*, 38: 545–605.

RAFFI, I. and BERNARDI, B. D. E, 2008. Response of calcareous nannofossils to the Paleocene–Eocene Thermal Maximum: Observations on composition, preservation and calcification in sediments from ODP Site 1263 (Walvis Ridge – SW Atlantic). *Marine Micropaleontology*, 69: 119–138.

RAFFI, I., BACKMAN, J. and PÄLIKE, H., 2005. Changes in calcareous nannofossil assemblages across the Paleocene/Eocene transition from the paleo–equatorial Pacific Ocean. *Palaeogeography, Palaeoclimatology, Palaeoecology*, 226: 93–126.

RÖHL, U, WESTERHOLD, T., MONECHI, S., THOMAS, E., ZACHOS, J. C. and DONNER, B., 2005. The third and final Early Eocene thermal maximum: characteristics, timing, and mechanisms of the "X" event. *Geological Society of America, Abstracts of Programs*, 37: 264.

SALAMY, K. A. and ZACHOS, J. C., 1999. Latest Eocene–Early Oligocene climate change and Southern Ocean fertility: inferences from sediments accumulation and stable isotope data. *Palaeogeography, Palaeoclimatology, Palaeoecology*, 145: 61–77.

SHAMRAI, I. A., 1963. Certain forms of Upper Cretaceous and Paleogene coccoliths and discoasters from the southern Russian Platform. Izvestiya Vysshikh Uchebnykh Zavedenii. *Geologiya i Razvedka*, 6: 27–40.

SHAMROCK, J. L., 2010. A new calcareous nannofossil species of the genus *Sphenolithus* from the Middle Eocene (Lutetian) and its biostratigraphic significance. *Journal of Nannoplankton Research,* 31: 5–10.

SHAMROCK J. L. and WATKINS D. K., 2012. Eocene calcareous nannofossil biostratigraphy and community structure from Exmouth Plateau, Eastern Indian Ocean (ODP Hole 762C). *Stratigraphy* 9:1, this volume.

SHIPBOARD SCIENTIFIC PARTY, 1990. Site 762. In*:* Haq, B. U., Rad, U. von, O'Connell, S. et al., *Proceedings of the Ocean Drilling Program, Initial Reports, Leg 122,* 213–288. College Station, TX Ocean Drilling Program,. doi:10.2973/odp. proc.ir.122.108.1990

SHIPBOARD SCIENTIFIC PARTY, 2000. Site 1123: North Chatham Drift– A 20–Ma Record of the Pacific Deep Western Boundary Current. In: Carter, R. M., McCave, I. N., Richter, C., Carter, L. et al., *Proceedings of the Ocean Drilling Program: Initial Reports, 181,* 1–184. College Station, TX Ocean Drilling Program. doi:10.2973/odp.proc.ir.181.107.2000

SIESSER, W. G. and BRALOWER, T. J., 1992. Cenozoic calcareous nannofossil biostratigraphy of the Exmouth Plateau, eastern Indian Ocean. *In*: Rad, U. von, Haq, B. U., Kidd, R. B. and O'Connell, S., *Proceedings of the Ocean Drilling Program: Scientific Results, 122,* 601–631. College Station, TX: Ocean Drilling Program. doi:10.2973/odp.proc.sr.122.162.1992

SLUIJS, A., BRINKHUIS, H., CROUCH, E. M., et al., 2008. Eustatic variations during the Paleocene–Eocene greenhouse world. *Paleoceanography*, 23: 18pp. PA4216. doi:10.1029/2008PA001615

STICKLEY, C. E., BRINKHUIS, H., MCGONIGAL, K. L., et al., 2004. Late Cretaceous–Quaternary biomagnetostratigraphy of ODP Sites 1168, 1170, 1171, and 1172, Tasmanian Gateway. In: Exon, N. F., Kennett, J. P. and Malone, M. J., *Proceedings of the Ocean Drilling Program: Scientific Results, 189*, 1–57. College Station, TX: Ocean Drilling Program. doi:10.2973/odp.proc.sr.189.111.2004

STRADNER, H., 1958. First report on the discoasters of the Tertiary of Austria and their stratigraphic use. In: *Proceedings of the Fifth World Petroleum Congress (New York, 1959) 1*: 1081–1095. New York: Fifth World Petroleum Congress, Incorporated, 1959.

———, 1959, Die fossilen Discoasteriden Österreichs. II Teil*. Erdoel Zeitschrift*, 75: 472–488.

TAN, S. H.1927. Discoasteridae incertae sedis. *Koninklijke Akademie van Wetenschappen te Amsterdam Proceedings*, 30: 411–419.

THOMAS, E., SHACKLETON, N. J. and HALL, M. A., 1992. Data report: carbon isotope stratigraphy of Paleogene bulk sediments, Hole 762C (Exmouth Plateau, eastern Indian Ocean). In*:* Rad, U. von, Haq, B. U. et al., *Proceedings of the Ocean Drilling Program: Scientific Results, 122,* 897–901. College Station, TX: Ocean Drilling Program. doi:10.2973/odp.proc.sr.122.195.1992

TOUMARKINE, M. and BOLLI, H. M., 1970. Evolution de *Globorotalia cerroazulensis* (Cole) dans l'Eocene moyen et superieur de Possango (Italie). *Revue de Micropaleontologie*, 13: 131–145.

VAROL, O., 1989. Eocene calcareous nannofossils from Sile (Northwest Turkey). *Revista Española de Micropaleontologia*, 21: 273–320.

VONHOF, H. B., SMITH, J., BRINKHUIS, H., MONTANARI, A. and NEDERBERG**,** A. J., 2000. Global cooling accelerated by early late Eocene impacts? *Geology*, 28: 687–690.

WEI, W., MCGONIGAL, K. L. and ZHONG, S., 2003. Data report: Paleogene calcareous nannofossil biostratigraphy of ODP Leg 189 (Australia–Antarctica Gateway). In: Exon, N. F., Kennett, J. P. and Malone, M. J., *Proceedings of the Ocean Drilling Program: Scientific Result, Leg 189,* 14pp. College Station, TX: Ocean Drilling Program. doi:10.2973/odp.proc.sr.189.103.2003

WEI, W. and WISE, S. W. Jr., 1990. Middle Eocene to Pleistocene calcareous nannofossils recovered by Ocean Drilling Program Leg 113 in the Weddell l Sea. In: Barker, P. F., Kennet, J. P. et al., *Proceedings of the Ocean Drilling Program: Scientific Results, 113,* 639–666. College Station, TX: Ocean Drilling Program. doi:10.2973/odp.proc.sr.113.125.1990

YOUNG, J. R. and BOWN, P. R., 1997. Proposals for a revisited classification system for calcareous nannoplankton. *Journal of Nannoplankton Research*, 19: 15-47.

YOUNG, J. R., GEISEN, M., CROS, L., KLEIJNE, A., SPRENGEL, C., PROBERT, I. and OSTERGAARD, J., 2003. A guide to extant coccolithophore taxonomy. *Journal of Nannoplankton Research, Special Issue* 1: 125pp.

ZACHOS, J. C., PAGANI, M., SLOAN, L., THOMAS, E. and BILLUPS, K., 2001. Trends, rhythms, and aberrations in global climate 65 Ma to present. *Science*, 292: 686-693.

Received February 22, 2012
Accepted August 9, 2012
Published September 30, 2012